THE ROLE OF NIX-MEDIATED MITOPHAGY IN MUSCLE STEM CELL FATE DECISION AND MUSCLE REGENERATION

JÉRÉMY RACINE

Thesis submitted to the University of Ottawa in partial Fulfillment of the requirements for the degree of Master of Science in Biochemistry

Department of Biochemistry, Microbiology and Immunology
Faculty of Medicine
University of Ottawa

ABSTRACT

Skeletal muscle is among the tissues displaying the greatest plasticity, attributable to a population of muscle stem cells (MuSCs). At basal conditions, MuSCs are in a standby state called quiescence. Once activated, they can either self-renew or commit toward myogenesis. This balance is required to mount an adequate repair response while maintaining long-term regenerative capacity. In this regard, mitochondria have emerged as important hubs for integrating signals and regulating stem cell behaviour. Mitophagy regulates mitochondrial properties through the autophagic degradation of organelles, suggesting an importance in MuSCs fate. Transcriptomic analysis of quiescent and activated MuSCs highlighted the Nix mitophagy pathway as a key player in quiescence maintenance. Nix is an important ubiquitin-independent mitophagy pathway in stem cell regulation. To test the role of Nix in MuSCs fate decision and muscle regeneration, we developed a conditional knock-out mouse model of Nix specific to MuSCs. First, we reveal that deleting Nix *in vivo* caused a significant decrease in mitophagy levels in quiescent and early-activated MuSCs. Next, using *in vitro* studies of culturing single myofibers, we show that Nix deletion alters MuSC fate decisions by causing premature and increased activation and commitment while depleting the MuSC pool. *In vivo* injury experiments further validate these observations, showing decreased self-renewal capacity post-muscle repair. We propose that dysregulation of Nix-mediated mitophagy disrupts MuSC fate and lineage progression, ultimately leading to muscle impairment. This study sheds light on the intricate interplay between mitophagy and MuSC behaviour, offering insights into potential therapeutic strategies for muscle regeneration.

Keywords: Muscle stem cells, mitophagy, BNIP3L/Nix, muscle regeneration, myogenesis.

ACKNOWLEDGEMENTS

First, I would like to thank my supervisor, Dr. Yan Burelle, and co-supervisor, Dr. Mireille Khacho. Mireille, you opened up the world of medical science to me when you first took me into your lab as an undergraduate student at the beginning of your lab in 2018. Your contagious passion and love for science fueled my interest in research. I am truly grateful for all your support throughout my undergraduate and graduate journey. Yan, thank you for welcoming me into your lab during my undergrad and supporting my desire to pursue a master's degree. You created a fun and enjoyable environment to work and develop science. You are one of the kindest and most supportive people I know. I am extremely thankful to have had you as a professor, supervisor, mentor, and friend. Thank you for the time I spent by your side.

Next, I want to thank an important person in my academic journey, Dr. Alexanne Cueillerier. Dear Alexanne, you are an exceptionally talented scientist with a tremendous and contagious love for science. Since the day we met, I have always been able to turn to you for advice and support. Thank you for guiding me through important life decisions, encouraging me to pursue a master's degree, helping me in the lab even after you left, cheering me on when experiments weren't working, and being someone I could always rely on. I am extremely thankful to have had you as a colleague, mentor and friend. I wish you continued success in your career and hope our friendship lasts for many years to come.

Thank you to my partner in crime, Mah Rukh Abbasi. Having parallel projects gave me the great privilege of having you by my side during our master's. From adventurous moments in the lab to late-night experiments, troubleshooting sessions, and tea sessions, I am thankful for your companionship. I wish you the best for the future.

To other members of Burelle's lab, I thank Dr. George Cairns for helping design my project and for constantly supporting me throughout my master's. To our star behind the scenes, Nikita Larionov, for handling all the animal work, sample preparation, and numerous lab tasks, I could never thank you enough for your work and support. Thank you to other present and past lab members I had the honour to meet and work with: Melissa Gourlay, Maeve Dixon, Sophia Goldman, Maxime Cloutier, Anna Wang, and Amine Fouzar.

Thank you to my deskmate, Brett Vahkal, for all the support, laughs, and tears we shared in our closet/office. Thank you to all the members of 2117 who brightened my days: Brayden Perras, Dr. Kayleigh Beaudry, Dr. Nicolás Collao, James Vanhie, and Dr. Alex Green. Cheers to Ciara Pember, Steven Wades, Dr. Matthew Triolo, Dr. Chantal Pileggi, and Taylor Smith for crossing paths with me. Thanks to all my friends and family who have supported me during my graduate journey.

I want to acknowledge the Metabolomics Advanced Training and International Exchange Program (MATRIX-NSERC-CREATE) for financially supporting my research activities. A special shoutout to Dr. Mary-Ellen Harper, Dr. Steffany Bennett, and Claire Fong-McMaster for coordinating such a wonderful program. Your coordination is helping MATRIX students to successfully complete their graduate studies while growing their professional careers as scientists.

I thank the Louise Pelletier Histology Core (RRID: SCR_021737) and the Cell Biology and Image Acquisition Core (RRID: SCR_021845) for their services, supported by the University of Ottawa, the Natural Sciences and Engineering Research Council of Canada, and the Canada Foundation for Innovation. I also acknowledge the expert contribution of Fernando Ortiz from the Flow Cytometry & Cell Sorting Facility at Ottawa Hospital Research Institute for his work on FACS (RRID: SCR_023349).

TABLE OF CONTENT

LIST OF FIGURES

LIST OF TABLES

LIST OF ABBREVIATIONS

4EBP1	4E-protein binding 1
ACVS	Animal Care and Veterinary Service
AMBRA1	Autophagy and Beclin 1 Regulator 1
ATP	Adenosine triphosphate
bFGF	Fibroblast growth factor-basic
BNIP3	BCL2-interacting protein 3
BSA	Bovine Serum Albumin
CTX	Cardiotoxin
DAPI	4’,6-diamidino-2-phenylindole
DMD	Duchenne’s Muscular Dystrophy
DMEM	Dulbecco’s Modified Eagle’s Medium
ECM	extracellular matrix
EDL	Extensor digitorum longus
eMyCH	Embryonic myosin heavy chain
FACS	Fluorescence-activated cell sorting
FBS	Fetal bovine serum
FGF2	Fibroblast Growth Factor-2
FUNDC1	FUN14 Domain Containing 1
H&E	Hematoxylin & Eosin
HGF	Hepatocyte growth factor
HSC	Hematopoietic stem cells

IF	Immunofluorescence
KO	Knock-out
LIR	LC3 interacting region
MAPK	Mitogen-activated protein kinase
MDV	Mitochondrial-derived vesicle
MMP	Mitochondrial membrane potential
MRF4	Myogenic regulatory factor 4
mTORC1	mammalian target of rapamycin complex 1
MuRF1	Muscle ring finger-1
MuSCs	Muscle stem cells
Myf5	Myogenic factor 5
MyHC	Myosin heanvy chain
MyoD	Myoblast determination protein
MyoG	Myogenin
NaCl	Sodium chloride
OMM	Outer mitochondrial membrane
OXPHOS	Oxidative phosphorylation
PAR	Partitioning defective complex
PARL	Protease presenilin-associated rhomboid-like
PBS	Phosphate-buffered saline
PCP	Planar cell polarity pathway
PFA	Paraformaldehyde

pS6	phospho-S6
qPCR	Quantitative polymerase chain reaction
RBPJ	Recombining binding protein suppressor of hairless
ROS	Reactive oxygen species
Rptr	Raptor
Spry1	Sprouty1
TA	Tibialis anterior muscle
TRPC	Transient receptor potential channel
TSC1	Tuberous sclerosis 1
WT	Wild-type

CHAPTER 1: INTRODUCTION

1.1 Skeletal Muscle and Myogenesis Overview

Accounting for 35% to 45% of body mass, skeletal muscle is the most abundant tissue of the human body[1]. Being controlled by the somatic nervous system, there are more than 600 different muscles with various properties and functions. This tissue is made of aligned myofibers, blood vessels, nerves, and the extracellular matrix (ECM) and is surrounded by the fascia that englobes the myofiber bundle[2]. Myofibers are multinucleated and composed of striated contractile muscle cells[3]. The myofibrils contain actin and myosin filaments, and their interaction is responsible for the translation of chemical energy to muscle contraction[2,4,5].

Myogenesis is the sophisticated process by which muscle tissue is formed and developed[2,6–10]. It encompasses a series of cellular events involving the activation, proliferation, differentiation, and fusion of myogenic precursor cells, ultimately leading to the formation of mature muscle fibres[2,6,7,10,11]. Myogenesis phases can be divided into embryonic myogenesis and adult myogenesis. Embryonic myogenesis occurs during early embryonic development and is responsible for the initial formation of the skeletal muscle tissue[2,7,12,13]. During this stage, multipotent progenitor cells known as myoblasts proliferate, differentiate, and fuse to form myotubes, which subsequently mature into muscle fibres[2]. In contrast, adult myogenesis occurs postnatally and is primarily involved in muscle repair and regeneration in response to injury or exercise-induced damage[2,13]. In adult myogenesis, a specific population of stem cells population that is adjacent to mature muscle fibres becomes activated in response to stimuli such as injury or exercise[2,6,8,13]. These activated stem cells then proliferate, differentiate, and fuse to repair or

replace damaged muscle fibres, ensuring the maintenance of muscle integrity and function throughout life [2,6,8,13].

Skeletal muscle exhibits a remarkable adaptative potential, which is evident in muscle hypertrophy and increased strength through resistance training. Conversely, several diseases, such as cancer, heart failure, genetic myopathies and aging, can cause muscle atrophy and loss of function[14,15]. Muscle laceration, exposure to myotoxic agents and ischemia can lead to acute muscle injuries[16,17]. Apart from their high plasticity, skeletal muscles possess an exceptional regenerative capacity. In response to injury, skeletal muscles undergo regeneration to maintain function and size, and proper regeneration occurs even after multiple and severe injuries[4,18].

Following muscle injury and homeostasis disruption, three main phases lead muscle repair[16], muscle degeneration and (*i*) inflammation, (*ii*) regeneration, and (*iii*) remodelling phases. The first event subsequent to an injury is necrosis of the tissue. After the degeneration process has begun, neutrophils will infiltrate the lesion and secrete multiple pro-inflammatory molecules, initiating muscle repair[19,20]. Next, the recruitment of anti-inflammatory cells will balance the inflammatory response[21]. The inflammatory reaction is prominent in the first four days post-injury[16]. Muscular regeneration, initiated through myogenesis, will begin 4-5 days post-injury, peak at two weeks and gradually fade after 3-4 weeks[16]. The remodelling phase occurs later during myogenesis. Remodelling of the injured muscle includes the maturation or regenerated myofibers, the recovery of functional capacity and fibrosis with scar tissue formation[16]. Complete restoration of muscle structure and function occurs within a few weeks after a major injury[22].

Because myofibers are post-mitotic cells, myogenesis requires a specific and dedicated population of stem cells called muscle stem cells (MuSCs) or satellite cells.

1.2 Muscle Stem Cells

1.2.1 MuSCs overview

MuSCs/satellite cells are a subpopulation of stem cells that are dedicated to myogenesis, which are located in a specialized niche microenvironment between the basal lamina of the myofibers and the plasma membrane[3,23]. MuSCs are considered adult stem cells because they possess the ability both to self-renew, ensuring a stable stem cell population, and to differentiate into progenitor cells, facilitating tissue repair[2,24,25]. They constitute 2% to 10% of the total nuclei of a muscle fibre, representing 20,000 to 1,000,000 cells per gram of muscle[7,26]. More than 80% to 90% of MuSCs are located only a few micrometres from a blood vessel[27]. MuSCs are characterized by a high nucleus-to-cytoplasm ratio, small nucleus size, condensed interphase chromatin, and diminished organelle content[2,9].The proportion of MuSCs is influenced by various factors, including muscle type, age, and species. In example, slow oxidative muscles (type I) tend to have a higher concentration of satellite cells compared to fast glycolytic muscles (type IIa/b)[28].

The muscle stem cell niche is a complex microenvironment that guides the behaviour of MuSCs. Recent studies have unveiled the heterogeneity of satellite cells within the niche, challenging the conventional understanding of their unipotency, such as their ability to differentiate into brown adipocytes[29,30]. The niche, encompassing vascularization, neuromuscular junctions, myotendinous junctions, and interstitial cell populations, serves as a structural scaffold transmitting mechanical and chemical signals to MuSCs[31]. This orchestrated composition creates an environment that allows satellite cells to adapt responsively to external stimuli. As a dynamic regulator, the MuSC niche plays a crucial role in influencing satellite cell activation, proliferation, and differentiation during both homeostasis and skeletal muscle regeneration, ensuring a delicate balance in maintaining the stem cell pool and supporting tissue repair[2,32].

1.2.2 Developmental Origin of MuSCs and Embryonic Myogenesis

The beginning of embryonic development is marked by the formation of three main germ layers: the ectoderm, mesoderm and endoderm[2]. After subdivisions, the mesoderm is divided into lateral, intermediate and paraxial mesoderm[2]. The paraxial mesoderm will further develop along the anterior-posterior axis of the embryo to form the bilateral paired blocks, which are named somites[2,7]. Somites contribute to the formation of diverse tissues including vertebral bones, tendons, cartilage, dermis, and skeletal muscles[2,12]. Most skeletal muscles, with the exception of certain head muscles, originate from the dorsal region of the somites known as the dermomyotome[2].

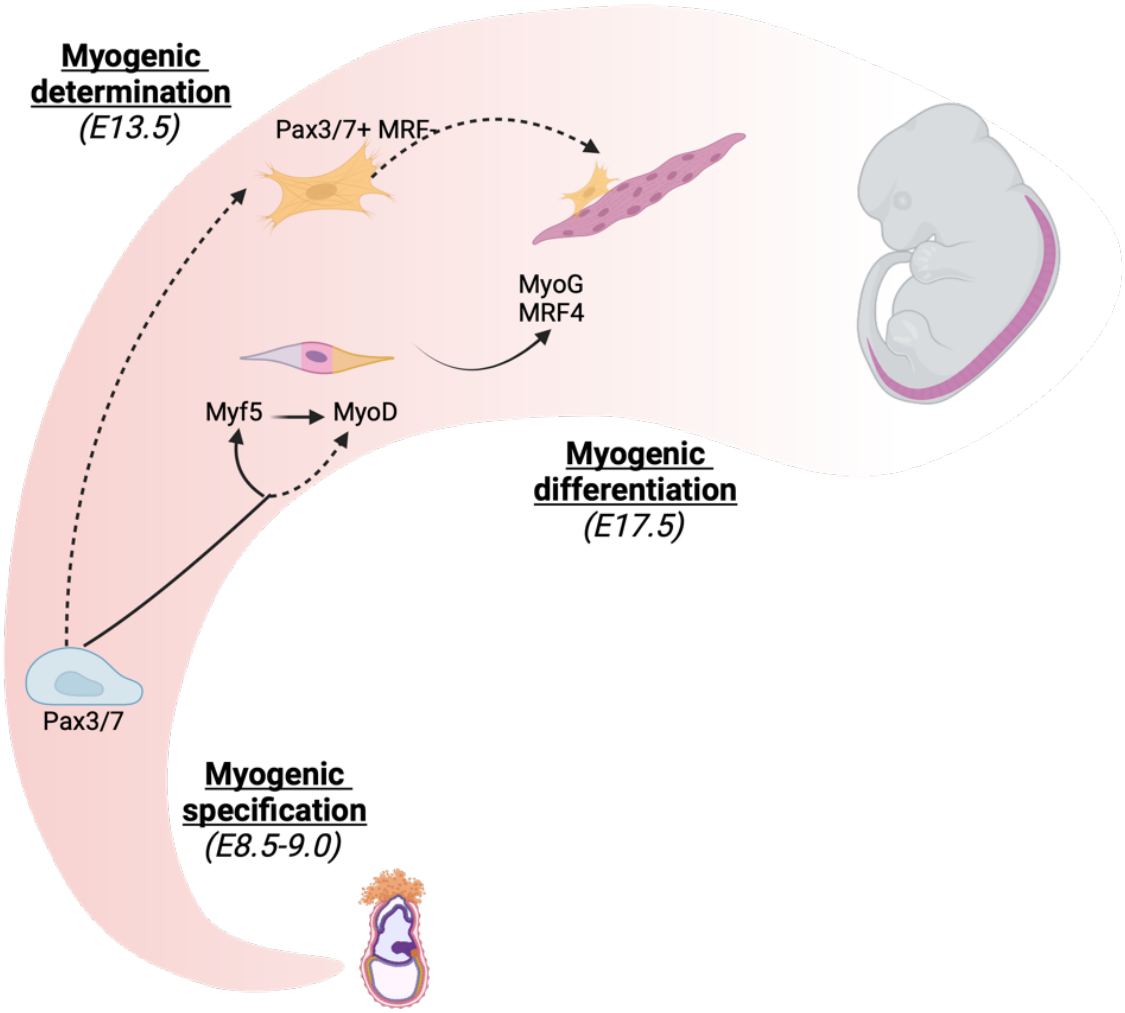

Figure 1. Embryonic development of MuSCs and Skeletal Muscle.

Myogenic specification begins at around E8.5-9.0 with the differentiation from the somites and the expression of Pax3 and Pax7. Pax3/7 will regulate the myogenic determination, by controlling the expression of the MRFs, Myf5 and MyoD, at E13.5. The upregulation of MyoG and MRF4 drives the myogenic differentiation at E17.5. A subset of Pax3/7 positive cells does not express MRFs and can generate satellite cells during late fetal myogenesis. Figure adapted from Dumont et al. (2015), Comprehensive Physiology[2]; and Deries et al. (2020), Springer Nature Switzerland[33]. Created using Biorender.

A comprehensive array of transcription factors regulates myogenic cells' specification, determination, and differentiation. Transcription factors within the paired box domain, specifically PAX3 and/or PAX7, are expressed in dermomyotome cells around E8.5-9.0 and serve as crucial upstream regulators in the formation of muscle tissue (**Figure 1**)[2,33]. Pax3 is essential for muscle development and the formation of the hypaxial domain, and its loss leads to the absence of the diaphragm and limb muscles[34,35]. It has been evidenced that Pax3 can target the hepatocyte growth factor (HGF) receptor c-met, a critical factor in the determination and migration of myogenic progenitors[36]. It has also been demonstrated that Pax3 regulated the embryonic expression of myogenic factor 5 (Myf5) and myoblast determination protein (MyoD), thereby initiating myogenic determination[37]. Although Pax3 plays a crucial role in muscle formation, its absence in postnatal muscles does not alter adult muscle regeneration[8,38]. In contrast, prenatal inhibition of Pax7 has milder effects on muscle development; its expression is indispensable for the formation of MuSCs[37,39–41]. Transcription activity of Pax7 is prominent to Pax3, and its ablation causes MuSCs depletion, reduction of fiber size, and impaired muscle regeneration, causing early postnatal death[42–44]. Using lineage experiments, it has been validated that Pax3-positive cells are necessary for embryonic myogenesis while Pax7-positive cells are deemed more critical for late fetal and postnatal myogenesis[45]. Altogether, it is suggested that Pax3-positive founder cells establish an initial fiber template, whereas Pax7-positive cells contribute to secondary fibres and MuSCs pool generation[7,46].

The myogenic determination (E13.5) and differentiation (E17.5) of the embryonic progenitors Pax3 and Pax7 are controlled by several myogenic regulatory factors (MRFs) (**Figure 1**)[2,33]. MRFs represent a family of basic helix-loop-helix transcription factors that include Myf5, MyoD, myogenin (MyoG) and myogenic regulatory factor 4 (MRF4)[2]. During the myogenic

determination phase, Myf5 is the first MRF to express in the epaxial domain and subsequently in the hypaxial domain of the dermomyotome[47]. Later on, MyoD will be expressed in the epaxial and hypaxial domains (**Figure 1**)[47]. Myf5 and MyoD activities overlap, causing only mild effects on muscle development when one is knocked out[48–50]. However, ablating their expression simultaneously results in the complete ablation of skeletal muscle formation while also preventing myogenic differentiation and the expression of MyoG[2,50]. Mice lacking MyoG succumb shortly after birth due to profound and widespread muscle deficiency[51]. In parallel with MyoG, MRF4 has a partial role in late myogenic differentiation and a potential role in myogenic determination in the absence of Myf5 and MyoD[51–53].

Even if most Pax3/7+ cells during development express MRFs before committing to myogenic progenitors, there exists a subset of this population that proliferates without inducing the MRF cascade (**Figure 1**)[54,55]. However, evidence indicates that nearly all satellite cells transiently express MyoD during embryonic development[56]. Nevertheless, it has been proposed that late in fetal development, Pax3/7+MRF− cells align themselves with nascent myotubes and eventually assume the satellite cell position beneath the basal lamina in postnatal muscles[55]. Upon reaching nascent muscles, the majority of Pax3/7+MRF− cells downregulate Pax3 and promptly upregulate Myf5[54]. The presence of Pax7+Myf5- satellite stem cells in adult muscle may represent a lineage continuum originating from the Pax3/7+MRF− progenitors.

Overall, embryonic myogenesis is driven by the expression of MRFs, which mainly include Pax3, Pax7, Myf5, MyoG, and MRF4. Embryonic myogenesis shares several similarities with adult myogenesis, such as the transcription factors and signalling pathways that regulate the process.

1.2.3 MuSCs quiescence

Under basal conditions, MuSCs are in a dormancy state called quiescence. Quiescence is a transient cell cycle inhibition state and is defined by the G_0 state[2,10,14,31,57,58]. Quiescent stem cells exhibit low metabolism, low RNA content, and minimal DNA damage[59–61]. These characteristics are essential to maintain this state for extended periods until their activation is needed for tissue regeneration. MuSCs also exist in a primed quiescent state, the G_{Alert} state, characterized by larger size, heightened metabolic activity, increased intracellular ATP, and faster initial cell division compared to G_0 MuSCs[26,31]. The preservation of quiescence involves meticulous coordination of various processes and is tightly regulated by both external and internal factors[26,31].

1.2.4 Regulation of MuSC quiescence

Amongst the various regulation mechanisms of MuSC quiescence, the specifically close location of the cells to the basal lamina suggests the importance of the microenvironment of the niche in its regulation[62]. For instance, M-cadherin proteins are found both on the satellite cell and the myofiber membrane and interact together to anchor the cell[63]. In their absence, the adhesive connections linking the stem cell to the myofiber are disrupted, resulting in earlier activation[64]. There are also some adhesion molecules, such as α7- and β1-integrins, that engage with the basal lamina to reinforce the stability of the MuSCs[65]. Other examples of cell-surface markers that anchor the satellite cells to their quiescent position are CD34, Integrin a-7, VCAM and NCAM[24,64,66,67]. The myofiber can correspondingly release factors, such as Wnt4, to restrict the mobility of MuSC, preserving the quiescent state[68].

Intrinsic mechanisms are also crucial in MuSC quiescence regulation. The Notch pathway is the most well-known and characterized regulation pathway of MuSCs quiescence[69–71]. Notch is

highly active in quiescent MuSCs and is crucial. It involves the interaction between the Notch ligand Delta-1 at the fiber surface and the Notch Receptors on the cell membrane[72]. Through its actions, Notch initiates the activation of the Recombining binding protein suppressor of hairless (RBPJ) transcription factor, which prompts the activation of numerous genes such as Hes1, Hes5, Hey and HeyL[73]. Dysregulation of these mechanisms is associated with precocious activation and loss of quiescence maintenance that consequently leads to a depletion of the MuSC pool[25,69,70,74,75].

Another key pathway in quiescence regulation is Sprouty1 (Spry1), more specifically in the regulation of Fibroblast Growth Factor-2 (FGF2)[58]. Without Spry1, FGF2 encourages the transition from quiescence to activation[58,76].

1.2.5 Transition toward a primed quiescent state

As previously mentioned, quiescent MuSCs are heterogeneous in terms of the depth of their quiescence state. It is crucial for satellite cells to have a subpopulation that can rapidly exit quiescence after a stimulus to engage myogenesis[59,77]. The most quiescent state is termed $G_{0,}$ and the primed state is G_{Alert}. G_{Alert} satellite cells were first noticed by *Rando et al.* when they observed that MuSCs in the contralateral muscle of an injured animal had different cycling properties from those of a completely uninjured animal[77]. They later characterized this subpopulation of satellite cells as being of bigger size, with increased transcriptional activity, increased mitochondrial metabolism, and accelerated cell cycle entry compared to G_0-MuSCs[77]. Following the identification of this subpopulation of quiescent MuSCs, many pathways have been identified as playing a role in G_{Alert} regulation. A key and well-known mechanism that supports this dynamic transition is the mammalian target of the rapamycin complex 1 (mTORC1) signalling pathway, which acts in response to extrinsic cues[77–80]. The involvement of mTORC1 in the G_{Alert} transition

was first observed with the induction of phospho-S6 (pS6) in G_{Alert} cells, which is a surrogate of mTORC1 activity[77]. Supporting this mechanism, blocking the inhibition of mTORC1 through ablating the expression of tuberous sclerosis 1 (TSC1) pushed the quiescent MuSCs of uninjured animals to have the matching characteristics of G_{Alert} MuSCs[77]. While suppressing mTORC1 signalling through deleting the Raptor (Rptr) protein, an essential component of mTORC1, caused the contralateral MuSCs of an injured animal to be unresponsive and did not share the characteristics of normal G_{Alert} satellite cells[77]. Recent evidence also reveals the role of the GLI3 transcription factor in mediating mTORC1 signalling[81]. GLI3 deletion molecularly activates mTORC1, shifting the MuSCs toward the G_{Alert} state without injuries. Consequently, this led to more rapid cell-cycle entry, amplified proliferation while expanding the stem cell pool, improved self-renewal, and greater regenerative capacity[81].

All these notions underscore the heterogeneity of quiescent MuSCs and the critical importance of the G_0 and G_{Alert} states in muscle regeneration. The existence of distinct subpopulations, each with unique characteristics, suggests a sophisticated regulatory network within the quiescent niche. Transitioning from G_0 to G_{Alert} primes MuSCs for rapid activation upon stimulation facilitates their activation and engagement in myogenesis and tissue repair.

1.2.6 The hallmarks of MuSCs activation and muscle lineage

The progression of the myogenic lineage following muscle injury is a precisely orchestrated process. It begins with the activation of quiescent MuSCs (Pax7+, Myf5+/-), upon tissue damage[2,60,61,82] (**Figure 2**). The subpopulation of Myf5+ MuSCs (Pax7 and Myf5+) is in a preactivated state (G_{Alert}) pre-injury, which is characterized by increased transcriptional activity and readiness for activation[59,77]. Upon activation, MuSCs commit and become myoblasts or

myogenic progenitors (Pax7+, Myf5+, and MyoD+) (**Figure 2**), which undergo several rounds of proliferation before exiting the cell cycle and becoming myocytes[2,9,83–85]. Myocytes, characterized by the downregulation of Pax7 and the presence of MyoD and MyoG, represent an intermediate stage between proliferating myoblasts and mature myofibers[2,86,87]. During this transition, embryonic myosin heavy chain (eMyHC) is expressed, marking early muscle differentiation[2,88,89]. Additionally, MRF4 plays a crucial role in the myocyte stage, where it cooperates with MyoD and MyoG to regulate gene expression involved in muscle maturation and contractility[52,90–92]. The final stage of the myogenic lineage is the fusion of myocytes into mature polynucleated myofibers, characterized by the expression of mature myosin heavy chain (MyHC)[2,88,89]. Mature myofibers represent fully differentiated muscle cells capable of contractile function, marking the culmination of the regeneration and repair process following muscle injury[93–96]. Throughout this progression, the orchestrated activity of myogenic regulatory factors such as MyoD, myogenin, and MRF4 guides the differentiation process and ensures the successful regeneration of muscle tissue (**Figure 2**).

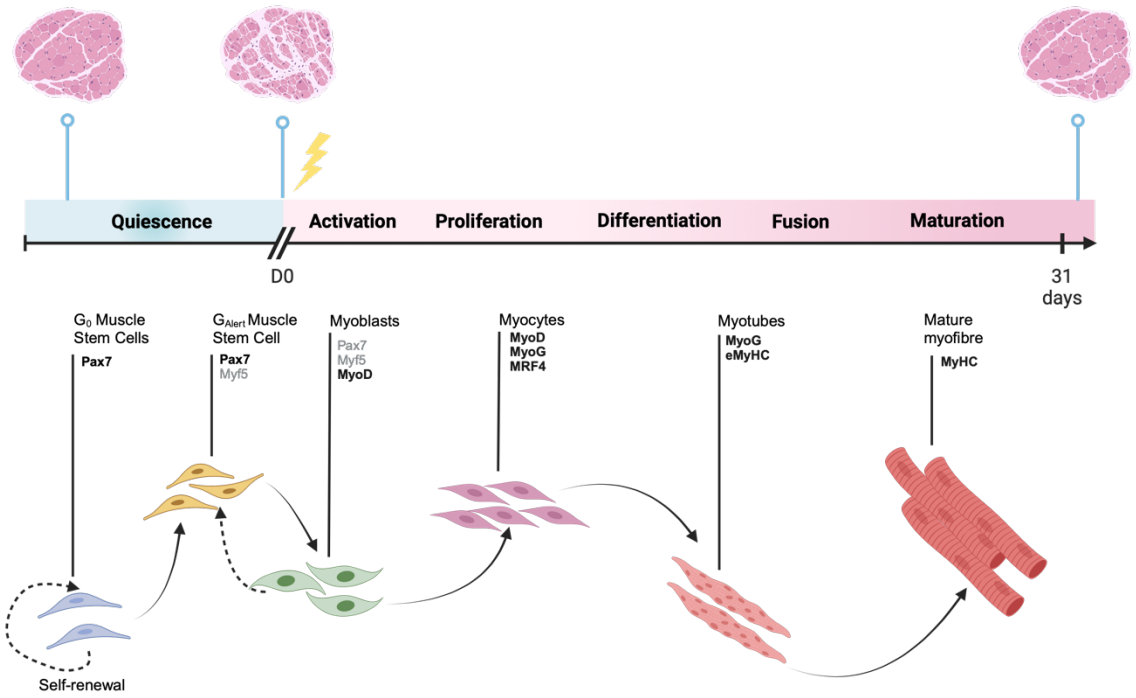

Figure 2. Progression of the myogenic lineage.

Upon muscle injury, dormant satellite cells (expressing Pax7+ and Myf5+/-) are stimulated and undergo differentiation into myoblasts (expressing Pax7+, Myf5+, and MyoD+). Following multiple rounds of division, myoblasts cease proliferation and transform into myocytes (marked by Pax7−, MyoD+, myogenin+, and MRF4+). Subsequently, myocytes have the capacity to fuse, forming multinucleated myotubes (expressing MyoG+ and eMyHC), which ultimately mature into myofibers (MyHC+). Additionally, a subset of satellite cells (expressing Pax7+ and Myf5−) possess the ability to self-renew, ensuring the replenishment of the satellite cell population. Figure adapted from Dumont et al. (2015), Comprehensive Physiology [2]; Schmidt et al. (2019), Cellular and Molecular Life Science [97]; and Garry et al. (2016) Methods in Molecular Biology [98]. Created using Biorender.

1.3 Adult Myogenesis; From MuSC Activation to Commitment and Differentiation

1.3.1 From quiescence to activation

After receiving a necessary stimulus, such as injury, exercise or a myopathy, MuSCs will exit quiescence to activate and re-enter the cell cycle, allowing the reparation of damaged muscle tissue[2,6,25,31,99]. The change of state is characterized by the shift from the G_0 phase to the G_1 phase of the cell cycle[100]. Re-entering the cellular cycle, plus the guidance of the basal lamina, prepares the MuSCs for myogenic programming through commitment, differentiation and proliferation. At this stage, committed MuSCs are termed myoblast and are expressing Pax7, and/or Myf5, and/or MyoD[2] (**Figure 2**). Overall, it takes approximately 25-40 hours for G_0 MuSCs to exit quiescence and advance through the G_1 phase for the first cellular division[61,101]. MuSC activation requires both signalling and transcriptional regulation.

1.3.2 Key Regulators of MuSC Activation

Following muscle activation, the ECM will release growth factors, such as FGF2, that can stimulate activation[102]. FGF2 triggers a rapid elevation of intracellular calcium levels via the Transient Receptor Potential Channel (TRPC), leading to NFATc2 and NFATc3 translocation into the nucleus, causing MuSC activation[103]. FGF2 also activates the p38alpha/beta mitogen-activated protein kinase (MAPK) pathway[104]. After activation, p38a/b MAPK translocates to the nucleus to inactivate tristeraprolin (TTP), stabilizing MyoD mRNA to promote satellite cell activation[31,57,105,106]. Additionally, the p38a/b MAPK signalling pathway is crucial for myoblast differentiation and fusion toward myotubes[107].

Nitric oxide (NO) is rapidly generated following tissue damage, exerting an immediate impact on satellite cell response and the inhibition of its synthase has been shown to diminish the

initial reaction of satellite cells to injury[108]. Moreover, NO has been found to stimulate the expression of matrix metalloproteinases and enhance the release of growth factors from the ECM[82]. Another key signalling regulator in muscle injury response is the cytokine TNF-α, which is rapidly produced and released post-injury[109]. Intriguingly, injection of TNF-α into healthy, uninjured muscles triggers satellite cell activation and entry into the cell cycle[109]. This activation occurs through the NF-kB pathway, as TNF-α activates NF-kB to silence the gene expression of Notch1, thereby promoting satellite cell activation[83].

Additionally, lipid mediator pathways, particularly involving Sphingosine-1-phosphate (S1P), play a role in satellite cell activation. S1P, derived from sphingomyelin metabolism in the plasma membrane, is abundant in the membrane of quiescent satellite cells[84]. Stimulation with S1P prompts satellite cell entry into the cell cycle, whereas inhibiting this pathway diminishes their response to mitogen stimulation[88].

During early muscle stem cell activation, notable changes in gene expression occur, marking a crucial step in the transition from a quiescent to an activated state[59,61]. With the aid of innovative techniques in the MuSC field, researchers have identified a spectrum of genes that undergo upregulation during this initial phase of activation [59,61]. For example, studies utilizing *in situ* fixation and nascent RNA labelling have revealed major transcriptional alterations in MuSCs immediately post-extraction, highlighting the activation-induced upregulation of genes associated with rRNA maturation, cell cycle entry, and the initiation of the myogenic program[61]. Additionally, a down-regulation of genes involved in fatty acid oxidation has been observed, consistent with the metabolic shift that MuSCs undergo upon activation[108].

These intricate signalling cascades and modifications to the transcriptional machinery highlight the multifaceted mechanisms underlying satellite cell activation and response to muscle injury.

1.3.3 Myogenic Differentiation Regulation

After undergoing multiple rounds of proliferation, myogenic cells exit the cell cycle and initiate the differentiation process. Subsequently, these cells either merge to create multinucleated myotubes or fuse with existing damaged fibres. The transition from proliferation to differentiation is governed by various signals and stimuli.

MyoD plays a pivotal role in driving myogenic progression and subsequent differentiation. Myoblasts lacking MyoD fail to elevate the expression of MyoG and MRF4, resulting in defective differentiation and compromised muscle regeneration[90–92]. MyoD aids in transitioning myoblasts from proliferation to differentiation by promoting the expression of cell cycle inhibitors like p21 and p57, and by stimulating myogenin expression[110,111].

Following MyoD, MyoG activates the expression of genes essential for muscle contractility, including myosin light chain, myosin heavy chain, muscle creatine kinase, α-actinin, troponin, and voltage-dependent calcium channel[95]. Similarly, MRF4, another myogenic regulatory factor, contributes to late-stage differentiation[52]. MRF activity is further modulated by the MEF2 family of transcription factors. For example, MEF2C interacts physically with either MyoD or myogenin, synergistically activating various muscle gene promoters[112]. Additionally, a positive feedback loop exists between MEF2 and MRF expression. Increased expression of MyoD or MyoG induces MEF2 expression, while overexpression of MEF2 reciprocally enhances MyoD expression, promoting myoblast differentiation[113,114]. Altering MEF2 expression results in

impaired myogenic differentiation and muscle regeneration and reveals compensatory mechanisms within MEF2 isoforms[115].

A switch from the Notch signalling pathway to the canonical Wnt signalling pathway is required to engage myogenic differentiation[116]. Various Wnt ligands are expressed in a temporally regulated manner during the myogenic lineage. During the early phase of regeneration, Wnt5a, Wnt5b, and Wnt7a expression are upregulated, while Wnt4 is downregulated[116,117]. The activation of canonical Wnt signalling, primarily mediated by the ligand Wnt3a, facilitates the differentiation of satellite cells, while the non-canonical Wnt signalling, driven by Wnt7a, promotes symmetric divisions of satellite cells, their migration, and the growth of myofibers[116,118–124]. In skeletal muscle, Wnt7a consistently signals through the Frizzled receptor Fzd7, activating multiple signalling pathways in both satellite cells and myofibers, including the planar cell polarity pathway (PCP) and the AKT/mTOR pathway[125].

Finally, specific microRNAs play a role in the shift from myogenic cell proliferation to differentiation. Notably, miR-1, miR-133, miR-206, and miR-486 are upregulated during myoblast differentiation and myotube formation, enhancing differentiation by directly inhibiting Pax7 transcription, which consequently results in increased MyoD activity[126–129].

Overall, myogenic differentiation is tightly regulated by key factors such as MyoD, MyoG, and MRF4, orchestrating the transition from myoblast proliferation to muscle cell differentiation. Additionally, the interplay between signalling pathways like Notch and Wnt further modulates this process, guiding myogenic progenitors toward maturation. These regulatory mechanisms ensure the timely expression of muscle-specific genes and the formation of functional myofibers during muscle regeneration and repair.

1.3.4 Myotube Fusion and Maturation

Following myogenic differentiation, myogenic cells must adhere together and undergo a cell-cell fusion that will change their shape and functions[130]. A recently discovered muscle-specific membrane protein named myomaker was shown to control myoblast fusion in mammalians[131]. The absence of myomaker in mice results in perinatal death attributed to the absence of multinucleated myofibers, and inducible deletion of myomaker in satellite cells significantly disrupts muscle regeneration after injury[131,132]. Interestingly, myomaker-deficient mice express normal levels of MyoD and MyoG, indicating that muscle precursor cells are able to commit into the myogenic lineage up to a certain point. Additionally, it was shown that MyoD and MyoG induce myomaker transcription and that to induce fusion, myomaker requires the rearrangement of cytoskeletal actin[131,132].

The fusion process can be categorized into early and late phases. Early fusion demands the interaction between myocytes, while late fusion involves the merging of myocytes with nascent multinucleated myotubes[2]. Although they share similarities, these two fusion modes engage distinct adhesion molecules and signalling pathways. For instance, myocyte-myocyte fusion is mediated by β1-integrin, leading to adhesion but not fusion in β1-integrin-deficient myoblasts[133–135]. On the other hand, myocyte-myotube fusion relies on proteins like FilaminC, which are associated with actin-binding[130]. In the late fusion phase, the expression of the calcium-activated transcription factor NFATc2 increases, subsequently regulating IL-4 expression. It is believed that IL-4 secretion is important in the final stage of myogenic fusion to attract additional myoblast[136]. Additionally, myotube interactions with the ECM become crucial for stimulating myotube formation during this stage. More specifically, it was demonstrated that laminin enhances myotube alignment and viability[137].

To become fully functional myofibers, nascent myotubes must undergo maturation, acquiring competent excitation-contraction coupling, contractile, and metabolic machinery[2]. The Akt/mTOR pathway plays a pivotal role in this process and hypertrophy, as the interaction between IGF-1 and its receptor activates Akt, subsequently stimulating mTOR downstream[93,94,138]. The Akt-1/mTOR pathway triggers various trophic effects through multiple pathways. For example, activation of mTOR stimulates protein synthesis by phosphorylating $p70^{S6k}$, which in turn activates ribosomal protein S6 while also exerting anabolic effects by inhibiting the translation repressor 4E-protein binding 1 (4EBP1)[139]. Akt supports hypertrophy by inhibiting FOXO activity, a factor involved in protein catabolism, thus preventing the induction of muscle ring finger-1 (MuRF1) and atrogin-1 expression, two E3-ubiquitin ligases associated with muscle wasting[140]. Although IGF-1 is the most well-known Akt/mTOR signalling activator, other proteins and growth factors can also induce this pathway. Notably, Wnt7a can stimulate satellite stem cell expansion and directly induce a hypertrophic response in myotubes through the Akt/mTOR pathway[122,124]. However, prolonged mTOR overstimulation triggers a feedback mechanism leading to muscle atrophy, underscoring the importance of tight regulation of the Akt/mTOR pathway for muscle hypertrophy[120].

In summary, myogenic fusion and maturation are essential processes in muscle development and regeneration. Myomaker, a recently identified muscle-specific membrane protein that governs myoblast fusion, is crucial for the formation of multinucleated myofibers. This process, orchestrated by the interaction of myocytes and nascent myotubes, involves distinct adhesion molecules and signalling pathways, highlighting the complexity of myogenic fusion. Moreover, myotube maturation, vital for acquiring functional myofibers, is regulated by the Akt/mTOR pathway, orchestrating various trophic effects essential for muscle hypertrophy. Tight

regulation of this pathway is critical to prevent muscle atrophy, underscoring its significance in muscle development and regeneration.

1.4 MuSC Fate Decision

1.4.1 Overview of Muscle Stem Cell Fate Decision

Respectively to their stemness traits, MuSCs have to determine upon activation if they will return to a quiescence state to replenish the MuSC pool (a process called self-renewal) or commit toward myogenic lineage[24,31]. The process of muscle stem cells choosing between self-renewal and commitment is known as stem cell fate decision. Maintaining a dynamic equilibrium during the fate decision to sustain the stem cell reservoir while meeting the demands of muscle regeneration is essential. Therefore, regulating the balance between self-renewal and commitment in muscle stem cells is crucial and tightly controlled.

1.4.2 Regulation of MuSCs Division

The regulation of the MuSC population involves a delicate balance between asymmetric and symmetric cell division pathways. Symmetric division can lead to either two differentiated daughter cells, resulting in stem cell exhaustion, or two daughter cells (**Figure 3**) maintaining stem cell properties, expanding the MuSC pool at the expense of muscle regeneration[2,25,31]. Asymmetric division yields one stem cell and a committed progenitor cell, which is crucial for MuSC pool maintenance and proper muscle regeneration[31].

The alignment of the cells is a critical factor influencing MuSC division. Planar division (parallel to the myofiber) generates daughter cells, expanding the stem cell pool (**Figure 3**). Meanwhile, apical-basal division (perpendicular to the myofiber) results in one daughter cell that

will replenish the MuSC population while the other cell commits toward myogenesis. Typically, in asymmetric division, the cell in proximity to the myofiber adopts Myf5 expression and commits to myogenesis, whereas the cell remaining attached to the basal lamina maintains Myf5 negativity and engages in self-renewal[24,25] (**Figure 3**).

Although the factors governing satellite stem cell fate are not fully elucidated, various factors and mechanisms are beginning to be uncovered. To begin, Myf5-positive committed satellite cells can undergo proliferation and differentiation after activation[141]. In contrast, Myf5-negative satellite stem cells possess the ability to self-renew through either symmetric or asymmetric division upon entering the cell cycle[2]. The regulation of Myf5 expression in Myf5-negative satellite stem cells during asymmetric division remains incompletely understood. Pax7, which induces Myf5 expression, requires methylation by Carm1 for this function[142,143]. However, in Myf5-negative satellite stem cells undergoing asymmetric division, Pax7 fails to interact with Carm1, leading to the suppression of Myf5 expression [142,143]. The orientation of muscle stem cell division within the satellite stem cell niche is significantly related to Myf5 expression. Cells dividing apically-basally mostly undergo asymmetric divisions, where the cell attached to the basal lamina remains Myf5-negative, while the one directed towards the myofiber becomes a Myf5-positive committed progenitor[141] (**Figure 3**).

In vitro studies demonstrate that the adherence of myogenic progenitor cells to the ECM influences their DNA segregation, with symmetrical adhesion leading to random segregation and asymmetrical adhesion favouring non-random segregation[144]. On ECM micropatterns, cells retaining old template DNA tend to localize to low adhesion areas, while committed cells localize to high adhesion areas. Interestingly, $Pax7_{hi}$ cells, which typically undergo asymmetric division,

are unaffected by ECM patterns, suggesting intrinsic factors play a role. However, applying these findings to satellite cells in their natural environment may be challenging, but they suggest that ECM adherence could influence muscle stem cell fate.

Multiple proteins have been identified to play roles during asymmetric division, exhibiting distinct localization preferences between the mother or daughter cells. The partitioning defective (PAR) complex, including PAR-3, PAR-6, and aPKC, polarizes in the committed daughter cell, activating p38α/β MAPK asymmetrically[99]. This activation induces MyoD expression, promoting commitment and proliferation of the daughter cell. The original template DNA, which is asymmetrical in the mother cell, colocalizes with Numb, a Notch signalling inhibitor[145]. However, some studies suggest Numb's asymmetrical location in the committed daughter cell[72]. Notch-3 is highly expressed in the mother stem cell, whereas the committed daughter cell expresses Delta-1, a Notch ligand[25]. Interactions between these cells reinforce their fate, and stimulating the Notch pathway in the mother cell maintains its stemness[25]. Overall, during asymmetric division, various proteins are differentially distributed between cells, influencing myogenic program activation through Myf5 and/or MyoD.

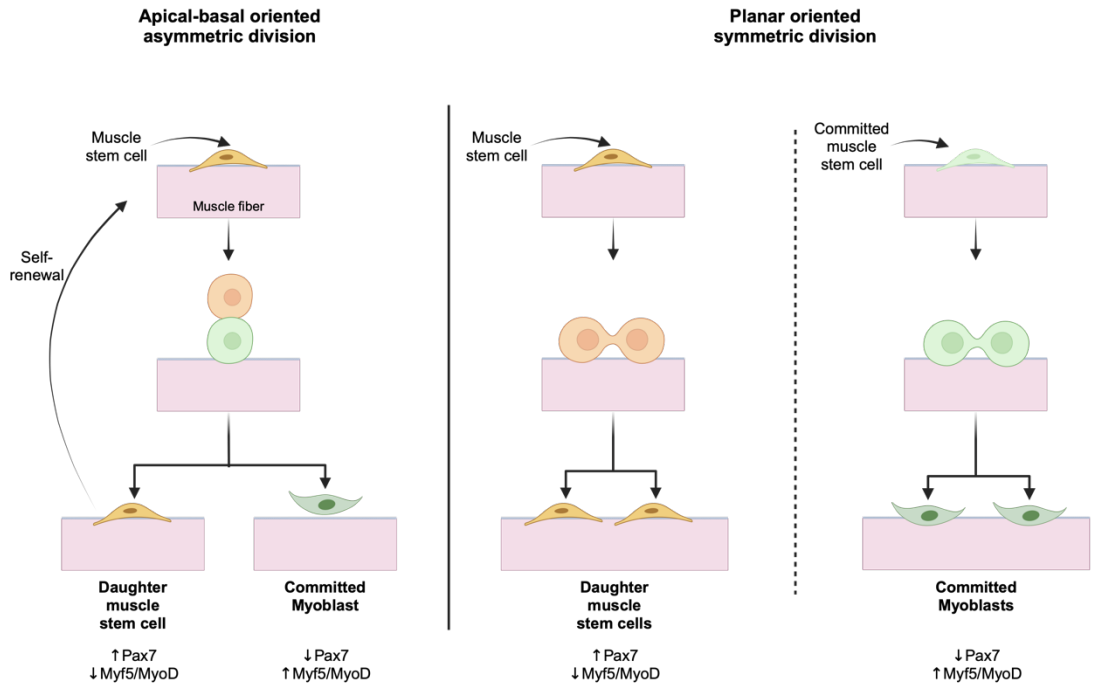

Figure 3. Regulation of MuSC division population through asymmetric and symmetric cell division pathways.

Symmetric division can either deplete the stem cell pool or expand it at the expense of muscle regeneration. Asymmetric division, crucial for MuSC pool maintenance, yields one stem cell and one committed progenitor cell. The alignment of cells, particularly planar and apical-basal divisions, plays a critical role in determining MuSC fate, with Myf5 expression dictating commitment to myogenesis. Figure adapted from Dumont et al. (2015). Created using Biorender

1.4.3 Consequences of Unbalanced MuSC Division

As previously mentioned, the destiny of muscle stem cells undergoes meticulous regulation upon activation, involving a sophisticated interplay of external and internal factors. This coordination aims to sustain the stem cell reservoir through adequate self-renewal while simultaneously generating myogenic progenitors essential for subsequent muscle regeneration. An imbalance in muscle stem cell fate determination can have adverse effects on muscle quality and

function. Such dysregulation is frequently observed in conditions characterized by muscle wasting and atrophy, contributing to their pathophysiology[76,141,146–148]. An example of imbalance toward committed MuSCs is the dysfunction in repopulating the MuSCs pool in aging and aged-induced sarcopenia. This imbalance results in a decline in the MuSC pool or stem cell senescence, ultimately impairing proper muscle repair and regeneration and consequently leading to a decrease in muscle mass and quality[76,148,149]. On the opposite, an imbalanced MuSC division toward self-renewal can also have catastrophic effects on muscle health, as is seen in Duchenne's Muscular Dystrophy (DMD)[150]. It's noteworthy that both age-induced sarcopenia and DMD exhibit similar characteristics, such as muscle atrophy and weakness, suggesting a potential connection between these diseases and their origins. While DMD was traditionally attributed to myofiber weakness, recent research highlights the crucial involvement of MuSCs in the DMD phenotype[150–152]. In DMD, the absence of dystrophin protein disrupts cell polarity and spindle orientation, resulting in a decrease in asymmetric divisions[141,153]. This disturbance leads to an excessive expansion of the stem cell pool at the expense of myogenic progenitors, ultimately discouraging muscle regeneration[153].

Altogether, these pieces of evidence underscore the critical importance of maintaining muscle health by achieving equilibrium during MuSC division. Therefore, it is imperative to deepen our understanding of the mechanisms governing MuSC fate decisions to shed light on related diseases and develop effective therapeutic strategies.

1.5 The Implications of Mitochondria in Stem Cells

1.5.1 Emerging Role of Mitochondria in Stem Cell Regulation

In recent years, mitochondria have emerged as crucial regulators not only in maintaining stem cell identity but also in orchestrating proper commitment and differentiation processes[154]. This newfound perspective suggests that the transition from quiescence to commitment is intricately linked to changes in mitochondrial properties defining cellular states[155]. Moreover, mitochondria have been recognized as pivotal players in cell growth and senescence, underscoring their significance in cellular homeostasis[154,155]. Their involvement in stem cell fate and function extends from healthy tissues to aging and disease contexts[156], with accumulating evidence indicating that damaged mitochondria and mitochondrial dysfunction contribute to stem cell aging, stress-induced aging, and cellular senescence[157,158]. Functionally, mitochondria serve as the primary site for crucial metabolic processes, generating adenosine triphosphate (ATP) through oxidative phosphorylation (OXPHOS) and producing reactive oxygen species (ROS) that play essential roles in cell signalling, particularly during quiescence maintenance and differentiation[159–161]. Thus, beyond energy production, mitochondria play integral roles in cell signalling and overall cellular homeostasis.

1.5.2 Mitochondrial Properties Defining Stem Cell States

Quiescent stem cells commonly exhibit a low metabolic rate, which is considered a conserved strategy to ensure long-term maintenance of potency and limit cellular damage[155]. The low energy demands during quiescence are reflected in the mitochondria characteristics, with their low content, simpler network and reduced cristae[162–164] (**Figure 4**). Recent studies, particularly on hematopoietic stem cells (HSCs), have highlighted the correlation between restricted oxidative

metabolism and stemness maintenance, with quiescent HSCs showing low mitochondrial activity compared to activated HSCs, based on their mitochondrial membrane potential[165] (MMP) (**Figure 4**). This metabolic regulation not only serves to protect against oxidative damage but also modulates ROS signalling, which is crucial for stem cell fate determination[162,163,166,167]. Low ROS levels preserve quiescence and self-renewal capacity, while increased ROS levels drive proliferation and differentiation [162,163,166,167].

It was shown that the morphology of mitochondria in hematopoietic, embryonic and mesenchymal stem cells appeared immature during quiescence, with spherical and fragmented with limited cristae development, often located near the nucleus[168] (**Figure 4**). However, a specific mitochondrial dynamic was recently uncovered within adult MuSCs. Quiescent MuSCs demonstrate elongated mitochondrial structures, which transition to smaller and fragmented forms directly upon activation, followed by mitochondrial elongation and increased mitochondrial mass during differentiation[169]. Additionally, it was revealed that a potent activation signal or elevated systemic factors at the injury site induce significant fragmentation, prompting stem cells to exit quiescence[169]. While MuSCs located farther from the injury receive a less intense stimulus, resulting in moderate fragmentation, leading to a primed state known as G-alert[169].

It has been well established that a metabolic switch is required for the passage from quiescence to activation, and commitment[164,170]. It has been numerously demonstrated that the subsequent energy demands for commitment are met through enhancing glycolysis and activating pyruvate oxidation[159,171–176]. This leads to a surge in mitochondrial ROS production, which are believed to act as an important signalling factor in stem cell commitment, acting with other metabolic cues[164,170]. Mitochondrial activation also alters the concentration of various

mitochondrial metabolites that modulate signalling pathways and gene programs crucial for fate determination and early differentiation, including NAD+/NADH, AMP/ATP, TCA cycle intermediates, Acetyl-CoA, and SAM/SAH[108,170,177–183].

Upon commitment to a particular lineage, progenitor cells undergo additional mitochondrial alterations to meet the specific demands of fully differentiated cells. Progenitors destined for differentiation into high-energy-demanding cell types like cardiac myocytes, skeletal muscle fibres, or neurons undergo remodelling characterized by heightened mitochondrial content and structural intricacy. This adaptation enhances OXPHOS capacity and bolsters antioxidant defences to manage electron leaks stemming from heightened metabolic activity[184–187] (**Figure 4**). Recent discoveries have highlighted the cruciality of mitochondrial fusion and the assembly of mitochondrial supercomplexes for MuSC differentiation[169,188].

Given the compelling evidence highlighting the role of mitochondria in shaping stem cell destiny, it encourages the investigation of how mitochondrial quality might influence stem cell fate.

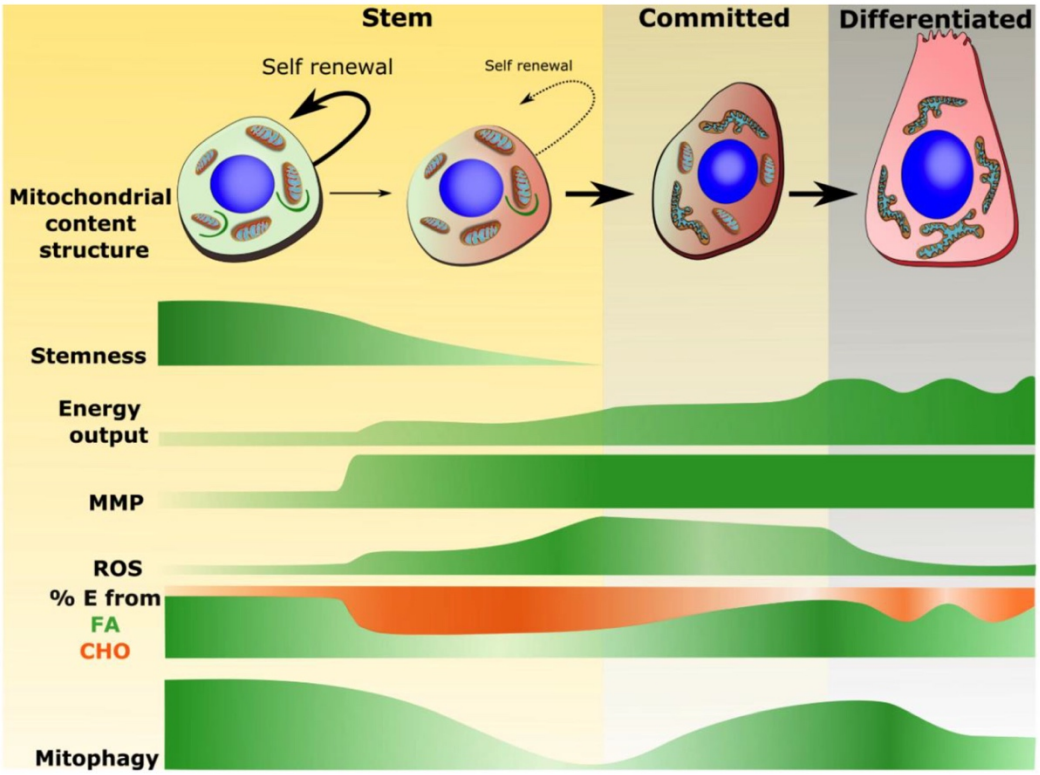

Figure 4. Illustrative overview depicting mitochondrial, metabolic, and mitophagy dynamics across stem cell lineage progression.

In the quiescent state, stem cells exhibit reduced mitochondrial content, simplified network structures, and fewer cristae folds, correlating with low metabolic activity and diminished ROS release. Subsets of stem cells with heightened stemness traits show lower MMP and ROS levels, favouring reliance on FAO. Conversely, stem cells with more active mitochondria display elevated MMP and metabolic rates, predisposing them to commitment upon activation. Mitochondrial ROS and other metabolic cues are implicated in driving stem cell commitment. Upon commitment, stem cells undergo lineage-specific mitochondrial remodelling characterized by increased biogenesis, network complexity, and OXPHOS capacity. Mitophagy plays a crucial role in maintaining metabolic stemness in quiescent stem cells and is upregulated during differentiation to facilitate mitochondrial remodelling. Reduced mitophagy is associated with stem cell commitment. (E, energy; FA, fatty acid; CHO, carbohydrate) Figure from Burelle et al. 2020, Biology.

1.5.3 Mitophagy, A Key Mitochondrial Quality Control Mechanism

Mitochondrial quality control comprises several pathways crucial for maintaining mitochondrial integrity, including the mitochondrial dynamics, mitochondrial protease and chaperone system, the mitochondrial-derived vesicle (MDV) pathway, and mitophagy[155,189,190]. Among these pathways, mitophagy has garnered significant attention due to its role not only in response to mitochondrial dysfunction and stress but also in developmental processes and tissue regeneration[155].

Mitophagy is a specialized form of autophagy that selectively targets and degrades mitochondria, distinct from the bulk degradation seen in general autophagy[191–196]. While general autophagy utilizes autophagosomes to deliver and degrade a variety of cellular components within lysosomes, mitophagy exclusively targets mitochondria for degradation[197,198]. This process serves as a critical mitochondrial quality control mechanism, responsible for the selective removal of damaged and dysfunctional mitochondria to maintain cellular homeostasis[191–196]. This process is facilitated by receptor proteins that link mitochondria to the autophagy membrane, allowing for their specific sequestration[191].

In mammals, mitophagy is divided into two main functional groups: PINK1/Parkin-dependent and PINK1/Parkin-independent mitophagy, based on the kinase PINK1 and the E3 ligase Parkin requirement[155,191]. Activation of mitophagy occurs during various physiological and pathophysiological conditions, including development, differentiation, and stress responses such as depolarization, oxidative stress, and hypoxia[155,199]. The process involves the sensing, sequestration, and trafficking of mitochondria to lysosomes for degradation, which can be stimulated through different mechanisms and signalling cascades. Both ubiquitin dependant- and

independent-mitophagy involve the binding to ATG8 homolog proteins of the LC3 and GA-BARAP subfamilies via a specific LC3 interacting region (LIR), facilitating the selective engulfment of mitochondria into autophagosomes[200]. Ultimately, fusion of the autophagosome with the lysosome leads to the elimination of targeted dysfunctional mitochondria[191,199].

1.5.4 The Role of PINK1-Parkin Mitophagy in MuSC Fate Decision

To better understand how mitophagy can dictate MuSC fate decisions, our lab started investigating the role of the most well-known and studied mitophagy pathway, PINK1-Parkin mitophagy[201–203], specifically in MuSCs. Under normal conditions, PINK1 is imported into mitochondria through the outer mitochondrial membrane (OMM), and rapidly degraded by the mitochondrial protease presenilin-associated rhomboid-like protein (PARL)[201]. However, during mitochondrial stress that causes depolarization of the mitochondria, PINK1 import is inhibited, leading to its accumulation on the OMM where it phosphorylates PARKIN, enhancing its ligase activity and substrate interaction[204–207]. PINK1 also phosphorylates substrates like MIRO, MFN1, and MFN2, promoting their ubiquitination by PARKIN[208–212]. Ubiquitination targets these proteins for proteasomal degradation and recruits autophagy adapter proteins BCRA1 and P62/SQSTM1, facilitating autophagosome formation near defective mitochondria[213–215].

Firstly, our lab highlighted the prominence of mitochondria colocalizing with autophagosomes in the MuSC quiescent state and the fact that activation drives the cells to downregulate mitophagy[216]. Then, using a germline PINK1 deficient mouse model, we demonstrated that altering mitophagy alters the MuSC fate decision[216]. More specifically, deleting PINK1 promotes the commitment of MuSCs upon activation, sacrificing their self-renewal capacity. This impairment causes a progressive loss of muscle regenerative capacity upon

injuries[216]. We also highlighted the liaison between the subsequent ROS increase and the cellular fate imbalance[216].

To better understand the role of PINK1-Parkin mitophagy in MuSC fate determination, we employed a conditional and inducible knockout strategy targeting Parkin specifically in MuSCs within a mouse model. Preliminary findings reveal that the absence of Parkin leads to an accelerated commitment of MuSCs *in vitro*, resulting in compromised self-renewal capabilities. Notably, Parkin-deficient MuSCs exhibit alterations in cell-cycle progression characterized by impaired proliferation and entry into the cell cycle. These *in vitro* observations were corroborated using a cardiotoxin injury model in an *in vivo* setting. Following injury, MuSCs lacking Parkin displayed enhanced commitment but impaired proliferation, ultimately leading to the depletion of the MuSC pool and diminished regenerative capacity.

1.5.5 Ubiquitin-Independent Mitophagy

Several mitophagy receptors operate independently of the PINK1-Parkin pathway, such as FUN14 Domain Containing 1 (FUNDC1), the BCL2-interacting protein 3 (BNIP3), the BCL2-interacting protein 3 like (BNIP3L or Nix), and Autophagy and Beclin 1 Regulator 1 (AMBRA1)[155,217]. To target a ubiquitin-independent mitophagy player in MuSC regulation, we analyzed an available transcriptomic dataset comparing *in situ* fixed MuSCs and 3-5h *in vitro* activated MuSCs[61]. Among the various mitophagy genes analyzed, we observed significantly higher expression of PINK1 and Parkin in quiescent MuSCs compared to activated cells[216]. Concurrently, BNIP3L/Nix gene expression also stood out as similarly expressed, suggesting it could also play a role in regulating mitophagy in the quiescent state.

1.5.6 Nix-Mediated Mitophagy

Nix, with a molecular weight of 19 kDa, is a receptor situated on the outer mitochondrial membrane and classified within the pro-apoptotic BCL2 subfamily[218]. This protein is widely distributed throughout various human organs and exhibits localization in both mitochondria and nuclei[219,220]. Initially recognized for its involvement in apoptosis[221], Nix has garnered attention for its pivotal role in orchestrating the extensive degradation of mitochondria during the maturation of red blood cells in reticulocytes, often in coordination with the anti-apoptotic protein Bcl-xL[222–224]. This function underscores its significance in cellular homeostasis and developmental processes.

The precise mechanism underlying Nix-mediated mitophagy remains a subject of ongoing investigation. However, it is known that Nix's engagement in mitophagy requires phosphorylation of its LC3-interacting region (LIR), facilitating interaction with LC3/GABARAP proteins[225–228]. Notably, dimerization of Nix at the outer mitochondrial membrane is critical for initiating mitophagy, suggesting a complex regulatory network governing this process[225]. Recent research highlights the potential importance of phosphorylation within Nix's C-terminal domain, particularly at serine residues 34/35, for efficient mitophagic activity[225,229].

In response to cellular stress, such as hypoxia, NIX expression is transcriptionally upregulated through the action of hypoxia-inducible factor 1 (HIF-1)[230,231]. This regulatory mechanism underscores Nix's adaptive role in mitigating cellular damage and ensuring survival under adverse conditions. Furthermore, Nix is proposed to interact with PARK2 for ubiquitination during PINK1/PARKIN-regulated mitophagy, implicating its involvement in both ubiquitin-dependent and independent mitophagy pathways[228].

While mitophagy primarily serves as a mitochondrial quality control mechanism for removing damaged organelles, the emerging role of Nix in orchestrating this process highlights its significance in cellular development and adaptation to environmental cues. Further exploration of Nix-mediated mitophagy promises to deepen our understanding of mitochondrial dynamics and their impact on cellular physiology and pathology.

CHAPTER 2: HYPOTHESIS AND AIMS

2.1 Rationale

Considering that ***i)*** specific mitochondrial characteristics are associated with stemness properties and myogenic lineage progression, ***ii)*** recent work emphasizes the role of mitophagy as a key regulator of MuSCs fate decision, ***iii)*** Nix mitophagic pathway is regulated in a similar way to Parkin and PINK1, ***iv)*** Nix interacts with the Parkin pathway; we make the hypothesis that Nix has a key role in MuSCs fate decision and muscle regeneration.

2.2 Hypothesis

More specifically, we hypothesize that **Nix is required to maintain quiescence and/or ensure muscular lineage progression by modulating the MuSC mitochondrial phenotype.**

2.3 Aims

To understand how Nix mitophagy regulates MuSCs fate decision and muscle regeneration, there are two experimental aims:

Aim #1: Study the effect of a Nix deletion in MuSCs on mitophagy

Aim #2: Determine the impact of *Nix* inactivation on MuSC fate decisions and muscle regenerative capacity.

1.1 Characterize the *in vitro* consequence of a MuSC-specific inducible KO of Nix on MuSCs fate decision using muscle fiber culture.

1.2 Characterize the *in vivo* impact of a MuSC-specific inducible KO of Nix on muscle regeneration and fate decision.

CHAPTER 3: MATERIALS AND METHODS

3.1 Animal Care and Generation of Conditional Nix Knockout Mice

All experiments on animals were approved by the Animal Care and Veterinary Service (ACVS) committee at the University of Ottawa and conducted according to the directives of the Canadian Council on Animal Care. Mice were maintained in ventilated cages in groups of 3-5 mice. Both sexes were kept on a regular 12h-12h light-dark cycle and had access to food and water *ad libitum*.

$Nix^{flx/flx}$ mice were obtained from Dr. Gerald W. Dorn and were previously described[223], where loxP sites flanked exon 4 through 6a. To study the effect of loss of Nix in Pax7+ cells, our team developed a Cre-flox conditional Nix by crossing the $Nix^{flx/flx}$ mice with Pax7 $CreER^{T2\ +/-}$ mice[232]. At 6-8 weeks of age, 200mg/kg of tamoxifen (Sigma T5648, 50 mg/mL dissolved in corn oil) was administrated via gavage to $Nix^{WT/WT}$-$Pax7Cre^{+/-}$ mice (wild-type, WT) and to $Nix^{flx/flx}$-$Pax7Cre^{+/-}$ mice (Nix KO). Tamoxifen was administrated daily for five days to activate cre-recombinase and was followed by a 10-day recovery period for efficient gene deletion.

All animals were genotyped at weaning via ear biopsies. DNA was extracted using the Extract-N-Amp Tissue PCR Kit (Sigma, XNAT2-1KT). After extraction, samples were amplified by PCR using the GoTaq Green Master Mix (Promega, M7123) and the primers described in Table 1. Confirmation of Nix KO was performed by quantitative PCR and immunostaining on FACS-sorted MuSCs.

Animals were used at 8-12 weeks of age for experiments and euthanized by cervical dislocation.

3.2 Cardiotoxin Preparation and Injections

Cardiotoxin (CTX) (Latoxan, L8102) was prepared in saline (0.9% NaCl) at a final concentration of 10 μM[233]. Nix KO and WT mice received a subcutaneous injection of Buprenorphine before the procedure and anesthesia by gas inhalation 30 minutes before CTX injection. Using an insulin-type disposable syringe, 50 μL of 10 μM CTX was injected 1-2 mm deep into the right tibialis anterior (TA) muscle. The uninjured contralateral TA was used as a control. After the injury, the mice recovered in a heated room and were transferred into a clean cage until harvesting.

All procedures were approved by the ACVS committee at the University of Ottawa and complied with the Canadian Council on Animal Care guidelines and the Animals for Research Act.

3.3 Muscle Tissue Harvest for Histology

At harvesting, mice were euthanized by cervical dislocation. After pulling the skin, the TA muscle was instantly dissected, weighted, and cut in half at the center in a cross-sectional orientation. Half of the TA was flash-frozen for 30 seconds in isopentane cooled in liquid nitrogen and then transferred to a -80°C freezer for storage. The second half was fixed in cold 2% (w/v) PFA (Sigma, P6148) for 30 minutes on ice while shaking. After fixation, TAs were washed twice in cold PBS and 0.25M cold Glycine, and then moved into 5% (w/v) sucrose for 2 hours and 20% (w/v) sucrose for 48 hours to allow tissue dehydration. Finally, the TAs were frozen in cold isopentane in liquid nitrogen for 30 seconds and stored at -80°C.

3.4 Single Myofiber Isolation and *In Vitro* Culture

The extensor digitorum longus (EDL) muscles of the lower legs were harvested immediately after cervical dislocation. They were digested in 0.5 % (w/v) collagenase B (Roche, 11088815001) and 1% (v/v) penicillin-streptomycin (P-S) (Wisent, 450-201-EL) for 45 minutes at 37°C. The EDL muscles were triturated in wash media (4.5 g/L glucose and 1% (v/v) P-S in DMEM) to separate the muscle into single myofibers. Every myofiber was washed trice and transferred either into culture or fixing well (timepoint 1 hour). Myofibers were cultured for 24-48-72-96 hours, depending on the experiment's purpose. The culture media used contained 4.5 g/L glucose, 20% (v/v) FBS, 1% (v/v) chicken embryo extract (MP Biomedicals, 092850145), 1% P-S and 7.5 ng/mL bFGF (Sigma, F0291-4X25UG) in DMEM unsupplemented media without phenol red. Cultured fibres were incubated at 37°C, 5% CO_2.

Myofibers were fixed using 2% (m/v) of warm PFA for 10 minutes, followed by three washes using PBS.

3.5 MuSCs Isolation

MuSCs were isolated by fluorescence-activated cell sorting (FACS) according to a published protocol[234]. Following cervical dislocations, muscles of the lower legs were harvested on ice for under 5 minutes and digested in 1% (w/v) Collagenase-B (Roche, 11088831001) and 0.4% Dispase II (Roche, 4942078001). Digestion used the Miltenyi MACS Octo-dissociator SLICE_FACS program for 7 minutes. After dissection, the muscle mixture was filtered with a 100 µm filter and centrifuged at 400g for 10 minutes to obtain a pellet. Cells were resuspended and incubated with red blood cell lysis (Sigma, R7757) for 5 minutes and washed with PBS before another centrifugation. The cells were resuspended into 1 mL of FACS buffer (3mM

ethylenediaminetetraacetic acid (EDTA), 10% (v/v) FBS in 1xPBS) and incubated with the conjugated antibodies, described in Table 2, for 30 minutes. The positive selection (α-integrin-7 and VCAM-1) was sorted by FACS at the Flow Cytometry facility at the Ottawa Hospital Research Institute.

3.6 Histology

3.6.1 Tissue Sectioning

Tissues were sectioned in a cross-sectional orientation at -25°C with a thickness of 14 µm using the HM525NX Cryostat (Louise Pelletier Histology Core, University of Ottawa). The tissue sections were placed on a charged slide (Fisher Scientific, 12-550-15) and were stored at -80°C until processing.

3.6.2 Hematoxylin & Eosin Staining

Flash-frozen tissue sections were first fixed in PFA for 30 minutes and washed thrice in PBS. The Louise Pelletier Histology Core then processed the slides at the University of Ottawa for hematoxylin and eosin (H&E) staining. Imaging was later performed on the EVOS FLAuto2 microscope at the University of Ottawa.

3.7 Immunofluorescence Staining

3.7.1 Tissue sections

Tissue sections used for immunofluorescence (IF) staining were fixed and dehydrated in sucrose before the cryo-sectioning. Tissues on slides underwent antigen retrieval (citrate buffer at pH=6.0) at the Louise Pelletier Histology Core. The samples were blocked in 3% (w/v) BSA for one hour. Tissues were incubated with primary antibodies overnight at 4°C, followed by three

washes with PBS. Finally, tissues were incubated with secondary antibodies for an hour at room temperature in the dark, then washed thrice before mounting. Primary and secondary antibodies are listed in Table 3. Invitrogen™ ProLong™ Gold Antifade Mountant with DAPI (ThermoFisher Scientific, P36935) and coverslip (Avantor, 48393-251). Slides were imaged on an EVOS FLAuto2 microscope.

3.7.2 Single Myofibers

Fixed myofibers were permeabilized in 0.1% (v/v) triton-x and 0.1M glycine in PBS for 10 minutes and blocked in 5% (v/v) horse serum, 2% (w/v) BSA and 0.1% triton-x in PBS for an hour at room temperature. Then the myofibers were incubated overnight at 4°C with primary antibodies in blocking solution, washed thrice and incubated for an hour at room temperature with secondary antibodies. Antibodies are listed in table 3. After washing, myofibers were mounted on slides using Invitrogen™ ProLong™ Gold Antifade Mountant with DAPI (ThermoFisher Scientific, P36935) and coverslip (Avantor, 48393-251).

3.7.3 MuSCs

At the selected time point, MuSCs were fixed for 15 minutes in warm 4% (v/v) PFA at 37°C and washed thrice with PBS. Cells were first quenched with 50 mM NH_4Cl for 10 minutes. After washing, MuSCs were permeabilized in 0.1% (v/v) for 10 minutes and blocked with 10% (w/v) FBS for 30 minutes. Incubation with primary antibodies occurred in 5% (w/v) FBS overnight at 4°C and with secondary antibodies at room temperature for an hour in the dark. Cells were incubated with DAPI antibody for 3 minutes at room temperature. Antibodies are listed in Table 3. After washing, myofibers were mounted on slides using Invitrogen™ ProLong™ Gold Antifade Mountant (ThermoFisher Scientific, P36934) and coverslip (Avantor, 48393-251).

3.8 Quantitative RT-PCR

Muscle stem cell pellets were processed for total RNA extraction using the PicoPure RNA isolation kit (Thermo Scientific KIT0204) following the manufacturer's protocol. The isolated RNA was then quantified using a nano-drop 2000 spectrophotometer and subjected to reverse transcription using the iScript Reverse Transcription Supermix for Rt-qPCR (Bio-Rad 1708840) according to the manufacturer's instructions. Subsequently, cDNA was synthesized using the SsoAdvanced Universal SYBR Green Supermix (Bio-Rad 1725271) as per the manufacturer's protocol. RT-qPCR was carried out using a CFX96 real-time PCR detection system at the University of Ottawa.

3.9 DNA sequencing

To confirm the mutations in the experimental model, DNA samples from mice were initially extracted and amplified following the genotyping protocol. Subsequently, the targeted PCR products were excised from the agarose gel under UV light to allow DNA extraction using the EZ-10 Spin Column DNA Gel Extraction Kit from Bio Basic (BS353). The extracted samples were then sent for sequencing to the DNA Sequencing Facility at StemCore Laboratories, located within the Ottawa Hospital Research Institute.

3.10 Statistical Analysis

Statistical analyses were conducted utilizing GraphPad Prism 8. Quantitative outcomes were expressed as means ± standard error of the mean (SEM). Differences in statistical significance were evaluated using an unpaired t-test for two groups and two-way analysis of variance (ANOVA) for multiple comparisons. Significance levels are denoted as follows: ns (not significant), *$p < 0.05$, **$p < 0.01$, ***$p < 0.001$, ****$p < 0.0001$. The minimum number of replicates per experiment varied across studies (Refer to individual figure legends for specific details).

Table 1. Primers for genotyping and quantitative polymerase chain reaction (qPCR).

Primer Name	Sequence		Method
	Forward	Reverse	
Cre	GAACCTGATGGACATGTTCAGG	AGTGCGTTCGAACGCTAGAGCCTGT	Genotyping
$Nix^{flx/flx}$	CACAGCATTGCCACCCCTGCAGAG	GCTGCAGATGCCGGGCCTGAGCAA	Genotyping
Nix deletion	CACAGCATTGCCACCCCTGCAGAG	ACCTGCCCATGCTCCAGAGCAGGC	Genotyping
HRPT	CAAACTTTGCTTTCCCTGGT	TCTGGCCTGTATCCAACACTTC	qPCR
TBP	CTTCCTGCCACAATGTCACAG	CCTTTCTCATGCTTGCTTCTCTG	qPCR

Table 2. Antibodies for MuSCs Isolation.

Antibody	Company/Cat. No.	Amount
PE rat anti-mouse CD31	BD Pharmingen 553373	2uL/mouse
PE rat anti-mouse CD45	BD Pharmingen 553081	2uL/mouse
PE rat anti-mouse CD11b	eBioscience 12-0112-82	2uL/mouse
PE rat anti-mouse Ly-6A/E (Sca1)	BD Pharmingen 553108	2uL/mouse
647-conjugated alpha integrin 7 (rat)	Ablab 67-0010-05	10uL/mouse
PE-Cy7-conjugated CD106 (VCAM)	Biolegend 105720	10uL/mouse
Optional: CD34-biotin + Strepdavidin-Cy7	CD34-Biotin: MACS 130-105-830 Strep-Cy7: eBiosciences 25-4317-82	10uL/mouse

Table 3. Antibodies for Immunofluorescence

Uses	Antibody	Company/Cat. No.	Dilution factor
Primary antibodies	Pax7 (mouse)	DSHB PAX7-S	1:14
	Pax7 (rabbit)	Invitrogen PA1-117	1:100
	MyoD (mouse)	SantaCruz sc-32758	1:50
	MyoG (mouse)	DHSB F5D	1:12
	Ki67(rabbit)	Abcam ab15580	1:500
	eMyHC (mouse)	DHSB F1.652-s	1:10
	BNIP3L/Nix (rabbit)	Cell Signaling D4R4B #12396	1:400
Secondary antibodies	Alexa-Fluor 488 (rabbit)	Invitrogen A11008	1:1000
	Alexa-Fluor 647 (mouse)	Abcam AB-150107	1:1000
	Alexa-Fluor 594 (mouse)	Invitrogen A11005	1:1000
	Biotin	Jackson 115-065-205	1:1000
	Cy3-Conjugated Streptavidin	Jackson 016-160-084	1:1000

CHAPTER 4: RESULTS

4.1 Mouse model development and validation

To determine the effects of Nix deletion in MuSCs, a mouse line was generated to have a conditional and specific knockout of the Nix gene in MuSCs. Pax7Cre$^{+/0}$ mice (*Pax7tm1(cre/ERT2)Gaka/+*) were bred with *Nix$^{flx/flx}$* mice (*B6-Bnip3Ltm1DorFl/Fl*). After multiple crossings, the resultant mice were *Pax7Cre-Nix$^{flx/flx}$* mice (*B6-Bnip3Ltm1DorFl/Fl-Pax7tm1(cre/ERT2)Gaka+/0*). After tamoxifen treatment, the Nix alleles are deleted in the MuSCs, resulting in an induced and specific knockout of Nix in Pax7^{+} cells.

Following the *Jackson Laboratory* breeding guidelines[235], a genotyping protocol with a three-target strategy was used and validated using DNA sequencing from genotyping products. **Figure 5a-b** visually demonstrates the primer strategy and the DNA sequencing results. Using the BLAST tool on the National Library of Medicine website, the DNA sequence from the PCR products demonstrated a 95% query cover score with the *Mus musculus targeted KO-first, conditional ready, lacZ-tagged mutant allele Bnip3l:tm1a(EUCOMM)Wtsi; transgenic* mouse. The sequence with the LoxP insert also successfully expressed the LoxP sequence[236], which is highlighted in **Figure 5b.**

To validate the gene knockout within MuSCs, MuSCs were first sorted using FACS. Then RNA was extracted to generate cDNA and quantify the gene expression using quantitative polymerase chain reaction (qPCR). Concurrently, cells underwent fixation and immunofluorescent staining for Nix to assess protein expression. The results illustrated in **Figure 5c-d** demonstrate a notable decrease in both gene and protein expressions.

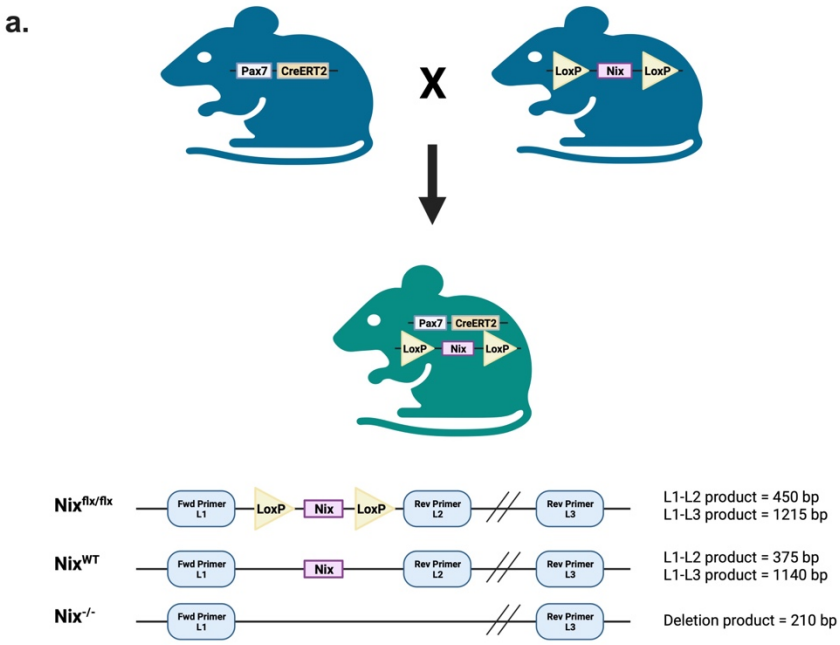
a.
Pax7
CreERT2
X
LoxP
Nix
LoxP
Pax7
CreERT2
LoxP
Nix
LoxP
Nix^flx/flx
Fwd Primer L1
LoxP
Nix
LoxP
Rev Primer L2
Rev Primer L3
L1-L2 product = 450 bp
L1-L3 product = 1215 bp
Nix^WT
Fwd Primer L1
Nix
Rev Primer L2
Rev Primer L3
L1-L2 product = 375 bp
L1-L3 product = 1140 bp
Nix^-/-
Fwd Primer L1
Rev Primer L3
Deletion product = 210 bp

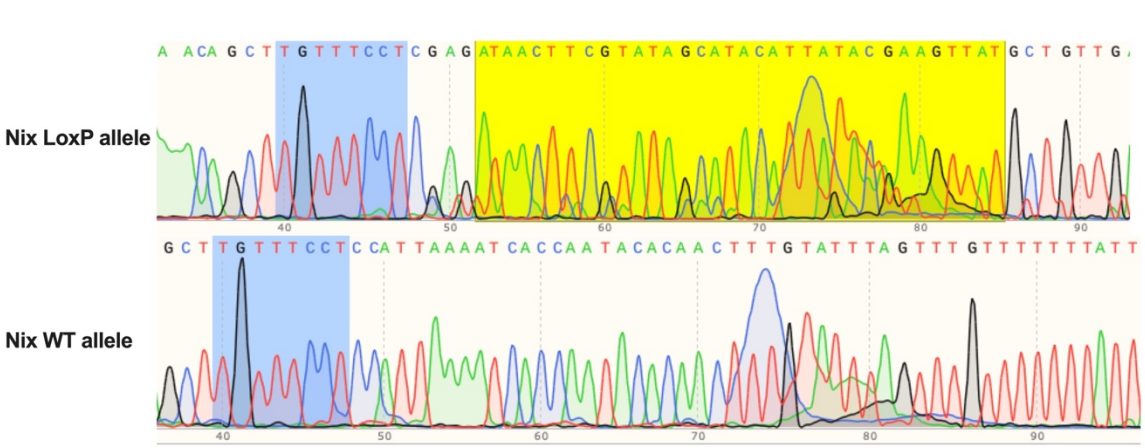
b.
Nix LoxP allele
Nix WT allele

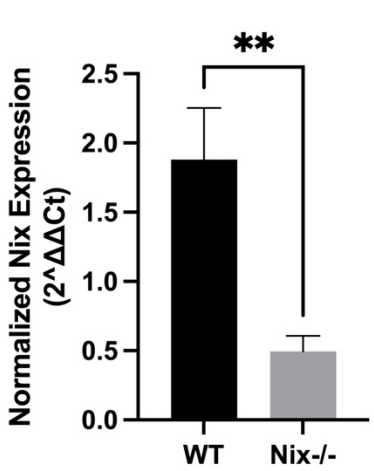
c.
**
Normalized Nix Expression (2^ΔΔCt)
2.5
2.0
1.5
1.0
0.5
0.0
WT
Nix-/-

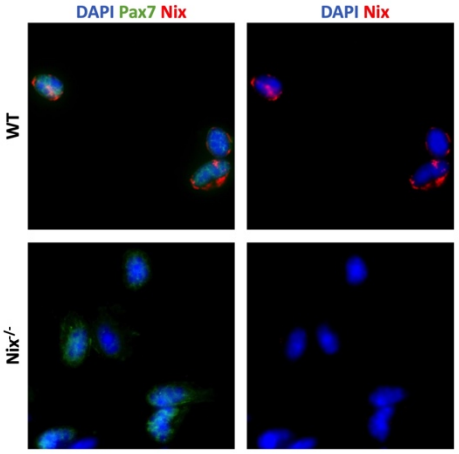
d.
DAPI Pax7 Nix
DAPI Nix
WT
Nix-/-

Figure 5. Validation of the conditional and inducible knock-out of Nix in MuSCs.

a. Visual representation of the breeding and genotyping strategy for the Pax7Cre-Nixflx/flx mice. b. Visual representation of DNA sequencing from genotyping products. The yellow highlight represents the LoxP sequence inserted after a reference point, highlighted in blue. c. Validation of Nix expression in WTs and Nix-/- MuSCs. Results were normalized to housekeeping gene Hypoxanthine-guanine phosphoribosyl transferase (Hprt) d. Qualitative protein expression of Nix in MuSCs. Immunostaining of Nucleus (DAPI), Pax7 (green) and Nix (red). Statistics were realised using an unpaired t test. Data is presented as mean ± SEM for n=4 mice per genotype. Statistical significance is displayed as *$p < 0.05$, **$p < 0.01$, ***$p < 0.001$, ****$p < 0.0001$.

4.2 Inactivating Nix decrease mitophagy levels within MuSCs

Single-cell mitophagy quantification was performed on freshly isolated MuSCs through FACS to quantify the effects of a Nix deletion on mitophagy levels. After isolation, cells were either immediately fixed (T0), cultured for four hours (T4), or treated with bafilomycin (Baf) for 4 hours. After fixation, mitochondria were labelled using TOM20 antibody and autophagosomes with LC3 antibody coupled with AlexFluor 488 and AlexFluor 594. The samples (n=3 mice per genotype) were imaged using high-resolution microscopy (Zeiss LSM880 AxioObserver Z1 with AiryScan FAST), followed by three-dimensional reconstruction and single colocalization quantification of mitochondria and autophagosomes. For each replicate and condition, 30-40 cells were analyzed.

At the basal quiescent state, mitochondria-lysosome colocalization was notably decreased in the $Nix^{-/-}$ population (**Figure 6b**). Inducing MuSC activation with a 4-hour incubation period showed a significant reduction in colocalization in both populations, even after inhibiting lysosome acidification using bafilomycin-A (**Figure 6b**). Additionally, colocalization was significantly reduced in the $Nix^{-/-}$ population after the bafilomycin-A treatment (**Figure 6b**). Notably, there were no discernible differences in mitochondrial content between the WT and $Nix^{-/-}$ groups across the experimental conditions (**Figure 6c**). However, in the quiescent state, the mitochondrial network appeared more fragmented in the $Nix^{-/-}$ population compared to the WT (**Figure 6d**). Despite similar levels of autophagosome content across conditions and genotypes, there was a substantial decrease in the size of individual autophagosomes observed upon activation in both groups (**Figure 6e-f**). This reduction in autophagosome size may indicate an early activation of lysosomal activity.

Given that blocking of lysosomal clearance using bafilomycin-A failed to elevate colocalization, and differences persisted between the two genotypes (**Figure 6b**), these results strongly imply that the diminished mitophagy predominantly contributed to the reduced colocalization upon activation, indicating impaired mitophagy due to Nix deletion.

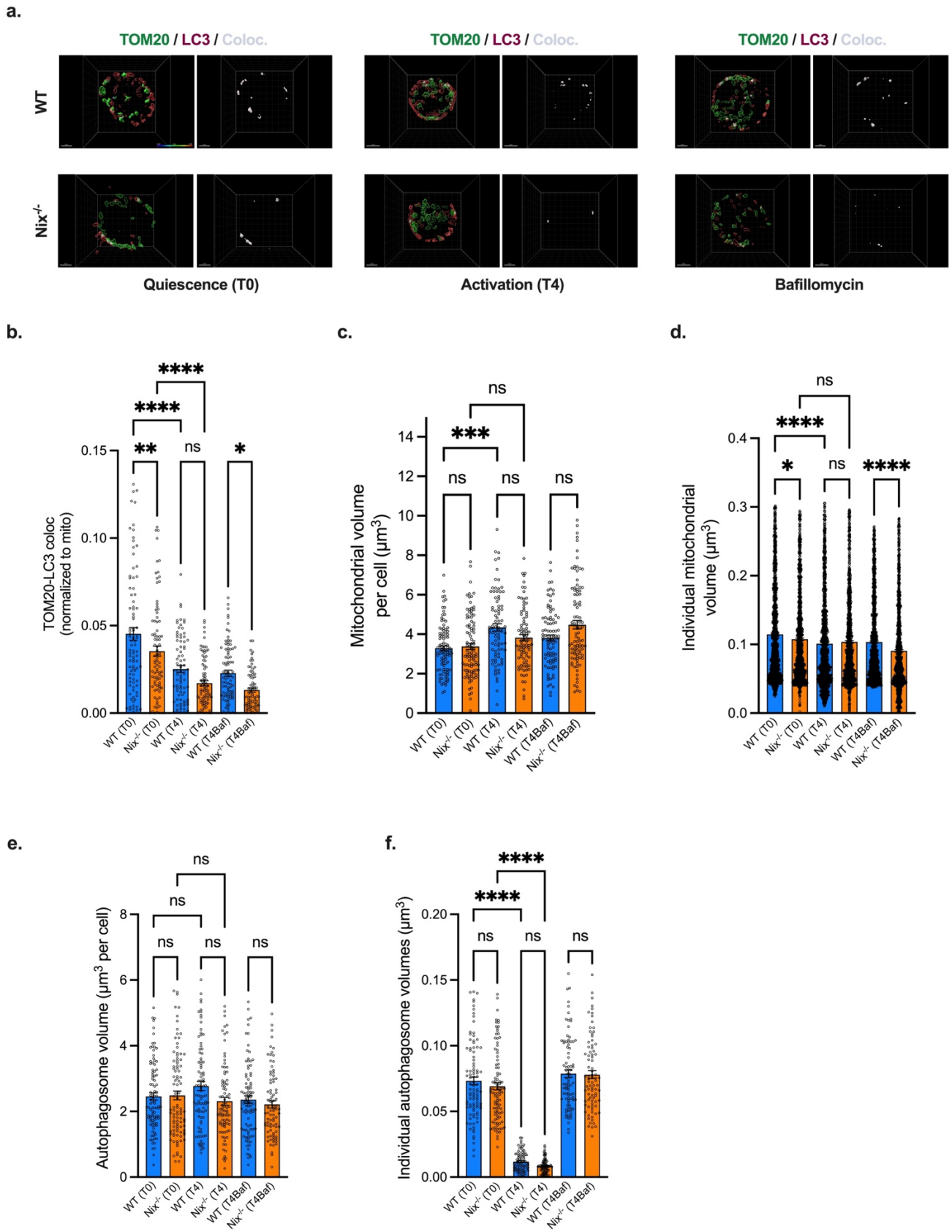
a.
TOM20 / LC3 / Coloc.
TOM20 / LC3 / Coloc.
TOM20 / LC3 / Coloc.
WT
Nix-/-
Quiescence (T0)
Activation (T4)
Bafillomycin
b.
TOM20-LC3 coloc (normalized to mito)
c.
Mitochondrial volume per cell (µm3)
d.
Individual mitochondrial volume (µm3)
e.
Autophagosome volume (µm3 per cell)
f.
Individual autophagosome volumes (µm3)
WT (T0)
Nix-/- (T0)
WT (T4)
Nix-/- (T4)
WT (T4Baf)
Nix-/- (T4Baf)

Figure 6. Single-Cell Mitophagy Quantification.

a. High-resolution microscopy images and Imaris 3D reconstruction of quiescent, activated, and Bafilomycin-treated MuSCs WTs and $Nix^{-/-}$. Cells were stained with TOM20 (green) and LC3 (red) to evaluate the colocalization of the objects (white). b. Colocalization of mitochondria and autophagosomes normalized to mitochondria volume at T0, T4h and treated with Bafilomycin (Baf). c. Total mitochondrial volume (μm^3) per cell. d. Individual mitochondria volume (µm3). e. Total autophagosome volume (μm^3) per cell. f. Individual autophagosome volume (µm3). Data is presented as mean ± SEM for 30-40 cells purified per mouse, from 3 mice per genotype. n_b = 80-91, n_c = 87-99, n_d = 1258-1317, n_e = 87-99 and n_f = 87-96. Statistics were realized using a one-way ANOVA test with data cleaned for outliers using the ROUT method. Statistical significance is displayed as *p < 0.05, **p < 0.01, ***p < 0.001, ****p < 0.0001.

4.3 Deletion effects of Nix promotes MuSC activation/commitment at the expense of self-renewal *in vitro*

To measure the effects of Nix deletion on MuSCs, the extensor digitorum longus (EDL) muscles were isolated and cultured *in vitro* for four days. Fibres were fixed directly after isolation (T1hr) and at 24-hour intervals. After fixation, the EDL fibres were permeabilized and incubated with key antibody markers for MuSCs quiescence and self-renewal (Pax7), activation (Pax7/MyoD), commitment (MyoD), and differentiation (MyoG) (**figure 7a**).

Directly after isolation, there were signs of earlier activation/commitment of the $Nix^{-/-}$ MuSCs with a significant decrease of the Pax7+ population (**figure 7b**). 24h post-isolation demonstrated a significant increase of the activated population (MyoD+ only). An increased commitment phenotype in the $Nix^{-/-}$ population was notable at 48- and 72- hours post-isolation by an increase in the Pax7-/MyoD+ cells. The propensity to activation led to an increased commitment of the $Nix^{-/-}$ MuSCs toward myogenesis at T72 and T96 with an increased proportion of MyoG+ population (**figure 7c**).

The impact of Nix deletion on MuSCs' cellular proliferation was initially assessed by quantifying the cell number per cluster (**figure 8a**), revealing that the heightened commitment did not alter the number of cells per cluster. Next, we measured cell-cycle re-entry using Ki67 staining on Pax7+ MuSCs (**figure 8b**), revealing that the number of Ki67+ cells was significantly higher in the $Nix^{-/-}$ population at T48 and T72 (**figure 8c**). Together these data would suggest that $Nix^{-/-}$ MuSCs are more prone to re-enter cell cycle but do not effectively divide and proliferate more than their WT counterparts, although a formal EdU staining would be required to confirm.

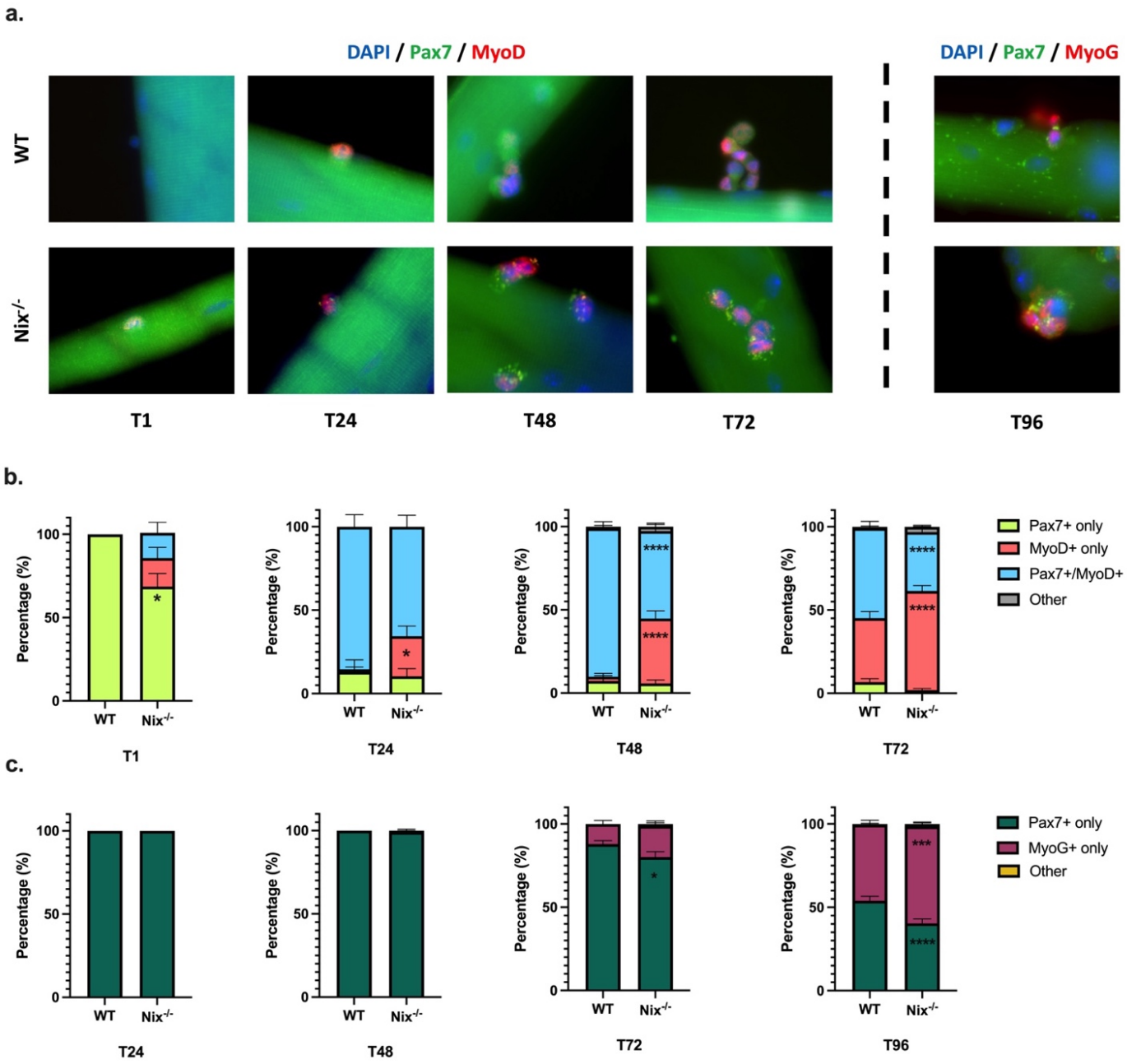
a.
DAPI / Pax7 / MyoD
DAPI / Pax7 / MyoG
WT
Nix-/-
T1
T24
T48
T72
T96
b.
Percentage (%)
WT
Nix-/-
Pax7+ only
MyoD+ only
Pax7+/MyoD+
Other
c.
MyoG+ only

Figure 7. Genetic inactivation of Nix promotes the MuSCs fate decision toward commitment while impairing the self-renewal process.

a. Representative immunofluorescence images of WT vs Nix-/- MuSCs on EDL single fibers at different isolation timepoints for Pax7, MyoD and MyoG. Magnification: 100X. b. Percentage of Pax7+, MyoD+ or Pax7+/MyoD+ cells per fiber in WTs vs Nix-/- EDL single fibers at T1, T24, T48 and T72 post isolation. c. Percentage of Pax7+ or MyoG+ cells per fiber in WTs vs Nix-/- EDL single fibers at T24, T48, T72 and T24, T48, T72, T96 post isolation. Data is presented as mean ± SEM for n=4 mice 3-5 fibers per mouse. Statistics were realized using a two-way ANOVA test. Statistical significance is displayed as *$p < 0.05$, **$p < 0.01$, ***$p < 0.001$, ****$p < 0.0001$.

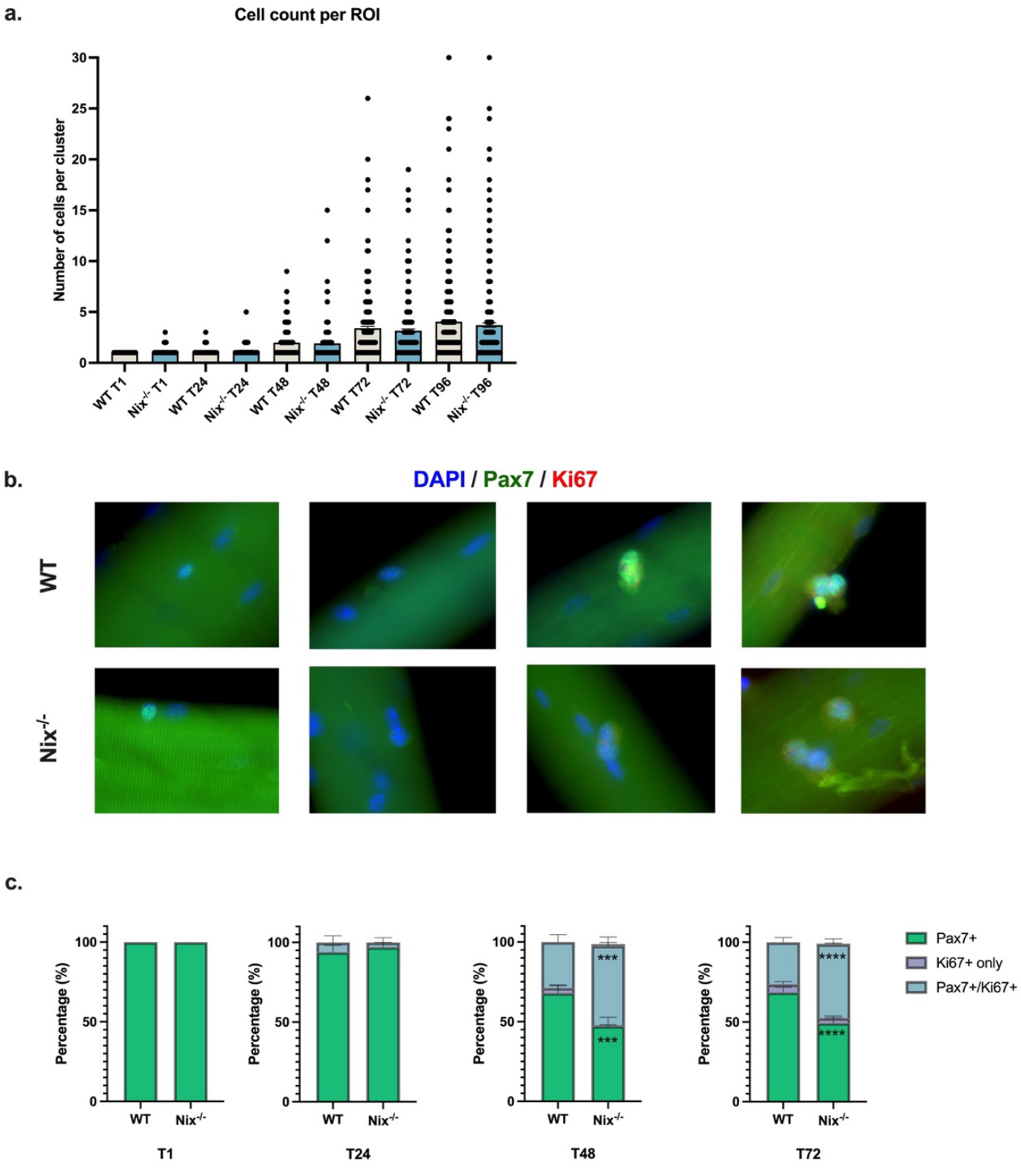
a.
Cell count per ROI
Number of cells per cluster
30
25
20
15
10
5
0
WT T1
Nix-/- T1
WT T24
Nix-/- T24
WT T48
Nix-/- T48
WT T72
Nix-/- T72
WT T96
Nix-/- T96
b.
DAPI / Pax7 / Ki67
WT
Nix-/-
c.
Percentage (%)
100
50
0
WT
Nix-/-
T1
T24
T48
T72
***
****
Pax7+
Ki67+ only
Pax7+/Ki67+

Figure 8. Increased cell-cycle re-entry in the Nix-/-.

a. Number of cells per cluster on EDLs (Pax7+/MyoD+/MyoG+), at various time points post-isolation (n=12). b. Representative immunofluorescence images of WT vs Nix-/- MuSCs on EDL single fibres at different isolation time points for Pax7 and Ki67. Magnification: 100X. c. Percentage of Pax7+, Ki67+ or Pax7+/Ki67+ cells per fiber in WTs vs Nix-/- EDL single fibres at T1, T24, T48 and T72 post isolation. Data is presented as mean ± SEM for n=4. Statistics were realized using a two-way ANOVA test. Statistical significance is displayed as *$p < 0.05$, **$p < 0.01$, ***$p < 0.001$, ****$p < 0.0001$.

4.4 Loss of Nix *in vivo* alters cell fate commitment and myogenesis upon injury

To study the consequences of Nix deletion on MuSC behaviour *in vivo*, muscle regeneration was studied using the cardiotoxin injury (CTX) model in the Tibialis Anterior (TA) muscle and immunofluorescent staining for Pax7 (**figure 9a**). Under normal uninjured conditions, there were no differences in the number of Pax7+ cells, indicating that deletion of Nix did not affect the baseline MuSC state and survival (**figure 9b**). 4 days post-injury (DPI), there was an important increase in the number of Pax7+ cells, in both WT and $Nix^{-/-}$ conditions consistent with increased proliferation in response to injury. Early in the myogenesis process, there was a tendency for a reduced number of Pax7+ MuSCs per fiber in the $Nix^{-/-}$ group (**figure 9b**). This trend became significant later on during regeneration, with the overall number of Pax7+ cells per fibre decreasing in $Nix^{-/-}$ at 7-, 14- and 21-DPI. At 4DPI, there was a significant decrease of committed MuSC per fiber (MyoG+) but with no differences at 7DPI (**figure 9d**). Finally, no differences in later differentiation at 4 and 7 DPI were measured by emHC immunostaining (**figure 9f**).

In contrast to the EDL data, in vivo injury resulted in decreased myogenin quantification four days after injury. These results indicating either an earlier activation or a decreased activation are not sustained by the quantification of eMHC, which remains unsignificant. This controversy can be explained by the poor condition of the muscle four days after injury, which complicates the visual analysis.

Altogether, the *in vivo* results on MuSCs' fate decision upon muscle suggest that deleting Nix in MuSCs slightly shifts the balance between self-renewal and commitment, reducing the stem cell population.

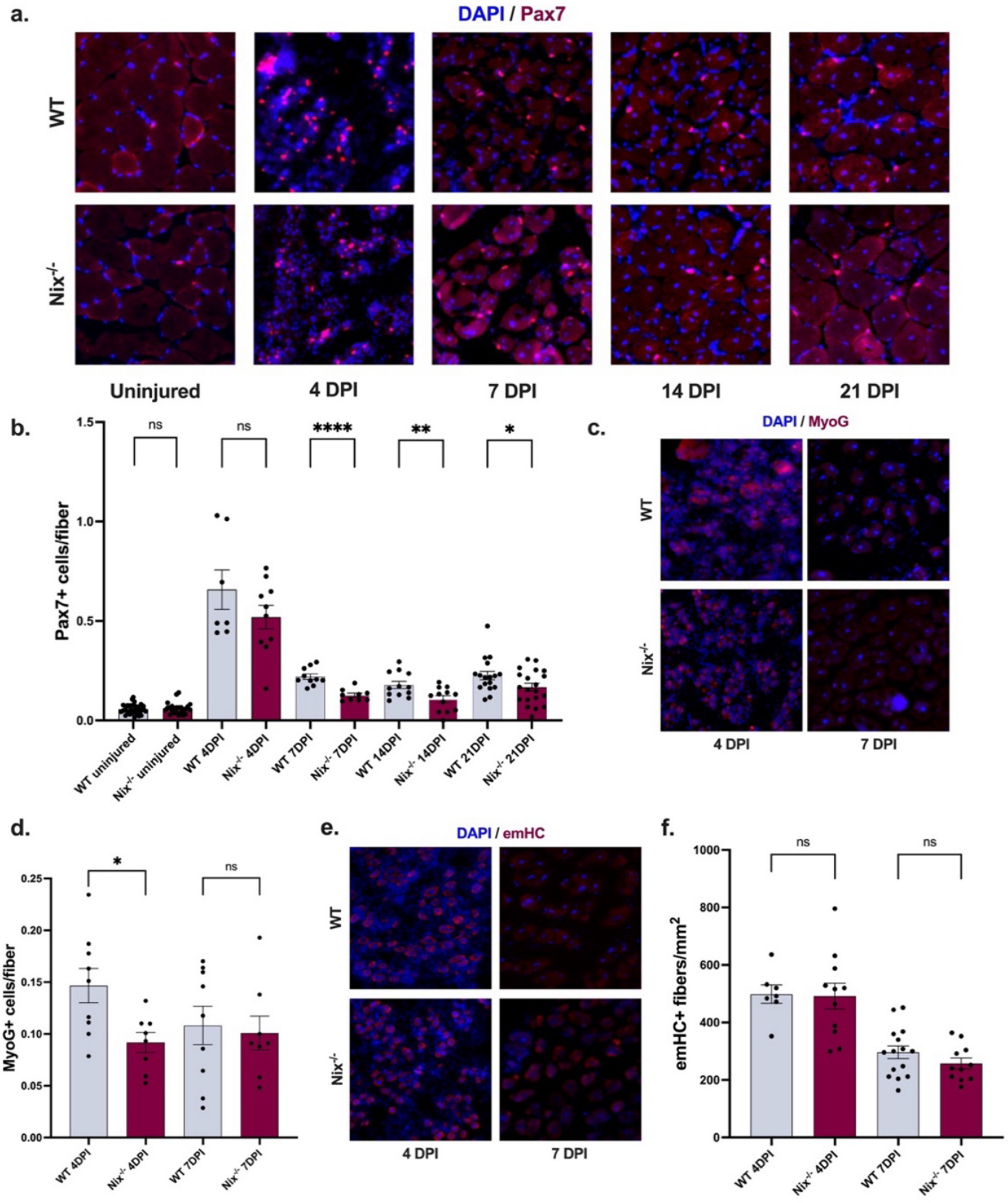
a.
DAPI / Pax7
WT
Nix-/-
Uninjured
4 DPI
7 DPI
14 DPI
21 DPI
b.
Pax7+ cells/fiber
ns
ns
****
**
*
WT uninjured
Nix-/- uninjured
WT 4DPI
Nix-/- 4DPI
WT 7DPI
Nix-/- 7DPI
WT 14DPI
Nix-/- 14DPI
WT 21DPI
Nix-/- 21DPI
c.
DAPI / MyoG
WT
Nix-/-
4 DPI
7 DPI
d.
MyoG+ cells/fiber
*
ns
WT 4DPI
Nix-/- 4DPI
WT 7DPI
Nix-/- 7DPI
e.
DAPI / emHC
WT
Nix-/-
4 DPI
7 DPI
f.
emHC+ fibers/mm2
ns
ns
WT 4DPI
Nix-/- 4DPI
WT 7DPI
Nix-/- 7DPI

Figure 9. In vivo effects of a Nix inhibition on MuSCs fate decision.

a. Representative immunostaining images of TA sections. Uninjured, 4-, 7-, 14- and 21 DPI stained for DAPI and Pax7. Magnification of 20X. b. Quantification of Pax7+ cells normalized per the amount of fiber for Uninjured, 4-, 7-, 14- and 21 DPI. c. Representative immunostaining images of TA sections. 4- and 7DPI stained for DAPI and MyoG. Magnification of 20X. d. Quantification of MyoG+ cells normalized per the amount of fiber for 4- and 7 DPI. e. Representative immunostaining images of TA sections. 4- and 7 DPI stained for DAPI and emHC. Magnification of 20X. b. Quantification of emHC+ fiber per mm2 for 4- and 7 DPI. Statistics were realised using an unpaired t test. Data is presented as mean ± SEM for n=6 mice per genotype. Statistical significance is displayed as *$p < 0.05$, **$p < 0.01$, ***$p < 0.001$, ****$p < 0.0001$.

4.5 Nix Ablation disturbs muscle regeneration upon injury

To determine the general effect of a Nix ablation on muscle regeneration, cross-sectional area (CSA) was measured on Hematoxylin and Eosin (H&E) stained sections of the TA muscle without injury and at 7-, 14- and 21 days post-injury (**figure 10a**). In the uninjured sections, there are no differences in the cross-sectional area across the groups, indicating that the Nix ablation did not alter the integrity of the muscles and the fiber size.

Altogether, no significant differences in mean fibre size were observed across genotypes after muscle repair (**figure 10b**). However, looking at fiber size distribution (**figure 10c-e**) there was a clear trend toward an increased proportion of bigger fibres in the $Nix^{-/-}$ group 21 days post-injury. We noted a similar phenotype in PINK1-deficient MuSCs[216]. However, this is contradictory to the decreased MyoG levels observed 4 days post-injury (**figure 9d**) but aligns with the *in vitro* results (**figure 7c**), implying higher levels of activation and commitment. The non-significance is perhaps due to the small group size (n=3) and variability across the samples. Therefore, the experiment needs to be repeated to conclude that ablating Nix mitophagy imbalanced muscle reparation.

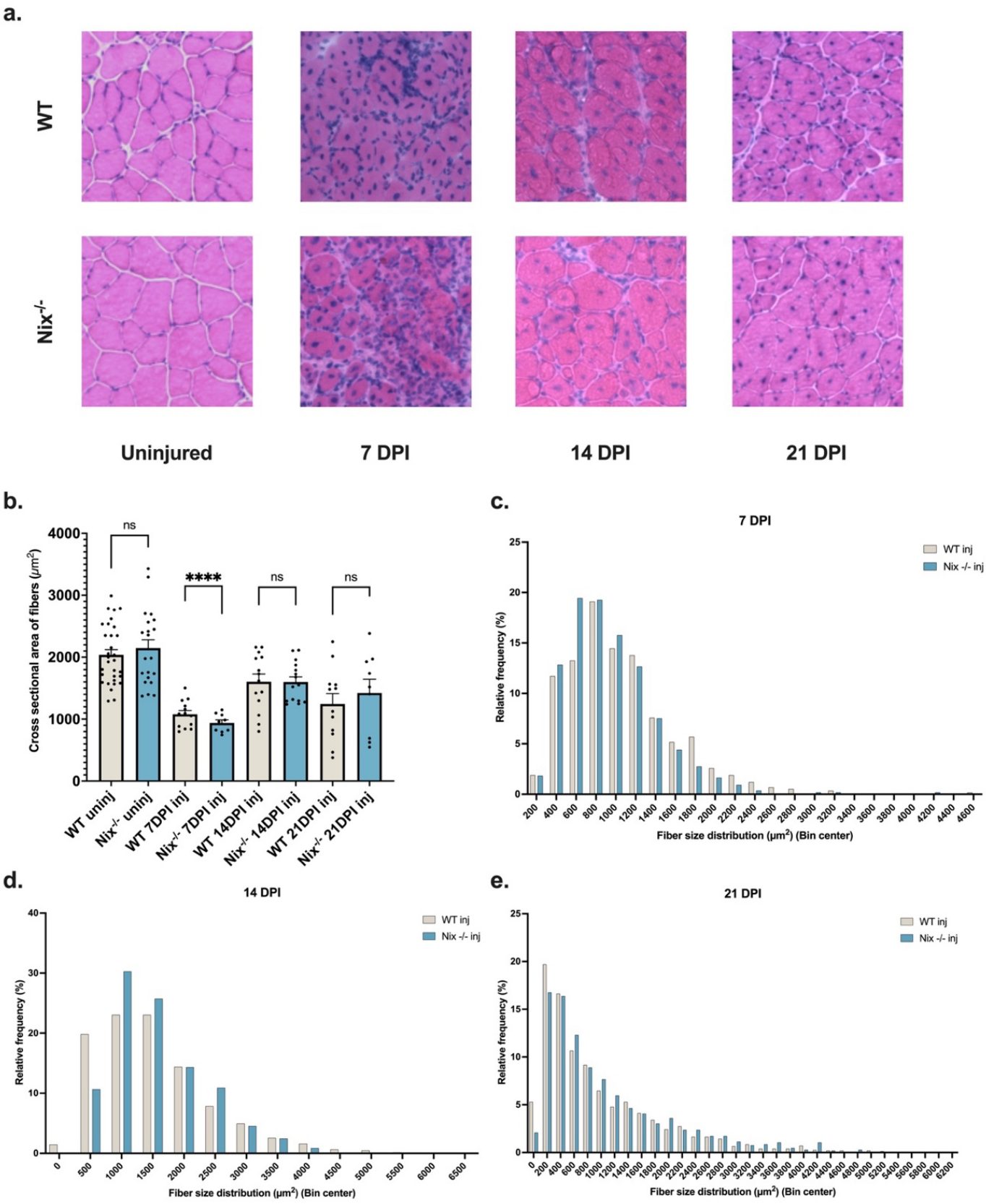
a.
WT
Nix-/-
Uninjured
7 DPI
14 DPI
21 DPI
b.
Cross sectional area of fibers (μm2)
ns
****
ns
ns
WT uninj
Nix-/- uninj
WT 7DPI inj
Nix-/- 7DPI inj
WT 14DPI inj
Nix-/- 14DPI inj
WT 21DPI inj
Nix-/- 21DPI inj
c.
7 DPI
WT inj
Nix -/- inj
Relative frequency (%)
Fiber size distribution (μm2) (Bin center)
d.
14 DPI
WT inj
Nix -/- inj
Relative frequency (%)
Fiber size distribution (μm2) (Bin center)
e.
21 DPI
WT inj
Nix -/- inj
Relative frequency (%)
Fiber size distribution (μm2) (Bin center)

Figure 10. In vivo effects of Nix deficient MuSCs on myogenesis.

a. Representative images of Hematoxylin and Eosin (H&E) stained section of the TA muscle without and at 7-, 14- and 21 days post-injury for WT and Nix-/- mice groups. Magnification at 20X. b. Cross-sectional area of fibers (µm2) for uninjured, 7-, 14- and 21 DPI. c. Fiber size distribution (µm2) at 7 DPI. d. Fiber size distribution (µm2) at 14 DPI. e. Fiber size distribution (µm2) at 21 DPI. Statistics were realised using an unpaired t test. Data is presented as mean ± SEM for n=4 mice per genotype for 7 DPI, n=5 for 14 DPI and n=3 for 21DPI. Statistical significance is displayed as *$p < 0.05$, **$p < 0.01$, ***$p < 0.001$, ****$p < 0.0001$

CHAPTER 5: DISCUSSION

5.1 Regulation of Mitophagy in MuSCs

Previous work from our lab has shown that quiescent MuSCs actively express mitophagy genes and exhibit a measurable mitophagy flux and prominent mitochondrial localization to $LC3^+$-$LAMP1^+$ autophagolysosomes, which rapidly decrease during activation.

Consistent with this data, we report that colocalization of mitochondria to $LC3^+$ autophagosomes is elevated in the quiescent state and undergoes rapid downregulation following 4h of spontaneous *in vitro* activation.

Furthermore, we also report that blocking lysosomal acidification with Baf-A during the activation period had no significant impact on mitochondrial colocalization to LC3+ autophagosomes, which supports the notion that inhibition of mitophagy rather than activation of lysosomal clearance is mainly responsible for the observed changes in colocalization during the transition from quiescence to activation.

Importantly, we provide novel evidence that Nix is expressed in the quiescent state and has a staining pattern consistent with mitochondrial localization. Furthermore, we report that genetic inactivation of Nix reduces mitochondrial localization to LC3+ autophagosomes by 16 %, suggesting that Nix is involved in the regulation of mitophagy in the quiescent state. No difference between genotypes was observed in the activated state, possibly because of the low mitophagy level observed in this condition.

In previous work on PINK1 and Parkin deficient mouse models, we reported similar partial ablation of mitophagy in quiescent MuSCs. Apart from the ubiquitin-dependent PINK1-PARKIN

mitophagy pathway, several ubiquitin-independent pathways have been reported[155]. Even if most of these pathways need to be defined, their overlaps is suspected to ensure proper homeostasis in case of dysfunction[217,237]. Such a regulatory overlap may explain why knock-out of a single pathway has a moderate effect of mitophagy and can be compensated by other evolutionarily conserved mechanisms.

The mechanisms by which Nix could regulate mitophagy in MuSCs remain to be defined. Based on current knowledge, it is likely that dimerization of Nix at the OMM and interactions between soluble LC3 and the LC3-Interaction Region (LIR) of Nix is required to engage mitophagy. Phosphorylation of the C-terminal domain of Nix was reported to promote its mitophagy-inducing ability, but the kinases and phosphatases involved currently remain unknown[225,229]. Nix is also thought to interact with PARK2 as a target for ubiquitination during PINK1/PARKIN-regulated mitophagy[228]. Further work will thus be required to clearly delineate the mechanisms of Nix-mediated mitophagy and potential interactions with the PINK1/Parkin pathway.

Interestingly, our data also reveal that genetic inactivation of Nix in MuSC also promotes mitochondrial fragmentation, an effect previously reported by our lab in PINK1-deficient MuSCs. At this point, it remains unclear whether this is a direct result of defective mitophagy *per se* or other effects on Nix or PINK1 deficiency in mitochondria. For instance, aside from its role in mitophagy, Nix is also known to play a role in the initiation of apoptotic signalling [238], which could also conceivably affect mitochondrial network morphology. Apoptotic signaling assays and analysis of the mitochondrial phenotype would clearly provide some insights.

5.2 Impacts of altering mitophagy genes on fate decision and myogenesis

Our analysis of fate decision using the EDL fiber culture model provides clear evidence that genetic inactivation of Nix promotes premature activation/commitment at the expense of self-renewal. This is evidenced by a decreased proportion of Pax7+ cells combined with an increased proportion of MyoD+ and MyoG+ cells.

Based on our count of the total number of MuSC (Pax7+, MyoD+ and MyoG+) per cluster at various time points, our results suggest that Nix deficiency has a limited effect on proliferation. Intriguingly, using the cell-cycle activity marker Ki67, we found evidence for precocious cell-cycle re-entry in Nix-/- MuSCs. Based on these results, we speculate that Nix deficiency predisposes MuSCs toward activation and cell-cycle re-entry without altering cellular division and proliferation. EdU assays will be required to confirm this hypothesis.

5.3 Impacts on Muscle Regeneration

By quantifying Pax7+ cells on the cross-section area of the TA muscle, we report that the symmetric cell division led to a partial *in vivo* depletion of the MuSCs pool after a single injury. However, preliminary data indicate that there are no negative effects on muscle repair after an injury. Conversely, there is a trend for bigger fiber sizes after the regeneration process. We noted a similar phenotype in PINK1-deficient MuSCs [216], where the initial partial depletion of the MuSC population led to ablated myogenesis after multiple injuries. With the similarity of the results, we hypothesize that multiple injuries in $Nix^{-/-}$ will lead to total depletion of the MuSC pool and, consequently, myogenesis failure.

CHAPTER 6: CONCLUSION

Previous work from our lab has shown that mitophagy is active in the quiescent state and rapidly decreased during activation, pointing to a role in the regulation of mitochondrial properties and MuSC function. In this project, we have successfully generated a novel model to study the regulation of mitophagy in MuSCs. We report that Nix is expressed in quiescent MuSCs, and that genetic inactivation of this mitophagy receptor reduces mitochondrial colocalization to autophagosomes, pointing to a role in the regulation of mitophagy in the quiescent state. We also report evidence that Nix deficiency impairs fate decisions by promoting premature activation/commitment at the expense of self-renewal, and preliminary evidence that this may contribute to impaired renewal of the MuSC pool in vivo and altered muscle regenerative capacity following injury.

Considering the overlap between various mitophagy-regulating pathways, additional work will be required to study the effect of depleting simultaneously ubiquitin-dependent and receptor-dependant mitophagy. To fully elucidate the effect of reducing Nix mitophagy on myogenesis, it is primordial to test the effects of repetitive injuries on muscular reparation. With the emerging role of mitochondria as integration and signalling hubs in stem cells, studying the consequences of accumulating dysfunctional mitochondria could provide new insight for drug therapies. Therefore, it is crucial to elucidate the effects of reduced Nix-mediate mitophagy on mitochondrial properties. This work could include ATP and ROS quantification, measurement of oxygen consumption further investigation on mitochondrial fragmentation and broader analysis of the cellular phenotype using Omics approaches.

CHAPTER 8: REFERENCES

1. Proctor, D. N., O'Brien, P. C., Atkinson, E. J. & Nair, K. S. Comparison of techniques to estimate total body skeletal muscle mass in people of different age groups. *Am J Physiol Endocrinol Metab* **277**, (1999).

2. Dumont, N. A., Bentzinger, C. F., Sincennes, M. C. & Rudnicki, M. A. Satellite cells and skeletal muscle regeneration. *Compr Physiol* **5**, (2015).

3. Fuchs, E. & Blau, H. M. Tissue Stem Cells: Architects of Their Niches. *Cell Stem Cell* **27**, 532–556 (2020).

4. Cornelison, D. D. W. & Perdiguero, E. Muscle stem cells: A model system for adult stem cell biology. in *Methods in Molecular Biology* vol. 1556 (2017).

5. Cretoiu, D. *et al.* Myofibers. *Adv Exp Med Biol* **1088**, 23–46 (2018).

6. Dhawan, J. & Rando, T. A. Stem cells in postnatal myogenesis: Molecular mechanisms of satellite cell quiescence, activation and replenishment. *Trends in Cell Biology* vol. 15 Preprint at https://doi.org/10.1016/j.tcb.2005.10.007 (2005).

7. Bentzinger, C. F., Wang, Y. X. & Rudnicki, M. A. Building Muscle: Molecular Regulation of Myogenesis. *Cold Spring Harb Perspect Biol* **4**, (2012).

8. Tajbakhsh, S. Skeletal muscle stem cells in developmental versus regenerative myogenesis. in *Journal of Internal Medicine* vol. 266 (2009).

9. Yin, H., Price, F. & Rudnicki, M. A. Satellite cells and the muscle stem cell niche. *Physiol Rev* **93**, 23–67 (2013).

10. Wang, Y. X., Dumont, N. A. & Rudnicki, M. A. Muscle stem cells at a glance. *J Cell Sci* **127**, (2014).

11. Stewart, C. E. & Jones, D. A. Myogenesis. *Encyclopedia of Exercise Medicine in Health and Disease* 621–624 (2012) doi:10.1007/978-3-540-29807-6_144.

12. Brent, A. E. & Tabin, C. J. Developmental regulation of somite derivatives: Muscle, cartilage and tendon. *Current Opinion in Genetics and Development* vol. 12 Preprint at https://doi.org/10.1016/S0959-437X(02)00339-8 (2002).

13. Hernandez-Torres, F., Rodríguez-Outeiriño, L., Franco, D. & Aranega, A. E. Pitx2 in embryonic and adult myogenesis. *Front Cell Dev Biol* **5**, 255569 (2017).

14. Argilés, J. M., Busquets, S., Felipe, A. & López-Soriano, F. J. Muscle wasting in cancer and ageing: cachexia versus sarcopenia. *Advances in gerontology = Uspekhi gerontologii / Rossiiskaia akademiia nauk, Gerontologicheskoe obshchestvo* vol. 18 Preprint at (2006).

15. Fitts, R. H., Riley, D. R. & Widrick, J. J. *Highlighted Topics Physiology of a Microgravity Environment Invited Review: Microgravity and Skeletal Muscle*. http://www.jap.org (2000).

16. Laumonier, T. & Menetrey, J. Muscle injuries and strategies for improving their repair. *Journal of Experimental Orthopaedics* vol. 3 Preprint at https://doi.org/10.1186/s40634-016-0051-7 (2016).

17. Karalaki, M., Fili, S., Philippou, A. & Koutsilieris, M. Muscle regeneration: Cellular and molecular events. *In Vivo* vol. 23 Preprint at (2009).

18. Yamakawa, H., Kusumoto, D., Hashimoto, H. & Yuasa, S. Stem Cell Aging in Skeletal Muscle Regeneration and Disease. *Int J Mol Sci* **21**, 1830 (2020).

19. Tidball, J. G. Inflammatory cell response to acute muscle injury. *Med Sci Sports Exerc* **27**, (1995).

20. Toumi, H. & Best, T. M. The inflammatory response: Friend or enemy for muscle injury? *British Journal of Sports Medicine* vol. 37 Preprint at https://doi.org/10.1136/bjsm.37.4.284 (2003).

21. Arnold, L. *et al.* Inflammatory monocytes recruited after skeletal muscle injury switch into antiinflammatory macrophages to support myogenesis. *Journal of Experimental Medicine* **204**, (2007).

22. Bentzinger, C. F., Wang, Y. X., Dumont, N. A. & Rudnicki, M. A. Cellular dynamics in the muscle satellite cell niche. *EMBO Rep* **14**, 1062–1072 (2013).

23. MAURO, A. Satellite cell of skeletal muscle fibers. *J Biophys Biochem Cytol* **9**, (1961).

24. Kuang, S., Gillespie, M. A. & Rudnicki, M. A. Niche regulation of muscle satellite cell self-renewal and differentiation. *Cell Stem Cell* **2**, 22–31 (2008).

25. Kuang, S., Kuroda, K., Le Grand, F. & Rudnicki, M. A. Asymmetric self-renewal and commitment of satellite stem cells in muscle. *Cell* **129**, 999–1010 (2007).

26. Hawke, T. J. & Garry, D. J. Myogenic satellite cells: physiology to molecular biology. *J Appl Physiol (1985)* **91**, 534–551 (2001).

27. Chiristov, C. *et al.* Muscle satellite cells and endothelial cells: close neighbors and privileged partners. *Mol Biol Cell* **18**, 1397–1409 (2007).

28. Gibson, M. C. & Schultz, E. Age-related differences in absolute numbers of skeletal muscle satellite cells. *Muscle Nerve* **6**, 574–580 (1983).

29. Asakura, A., Komaki, M. & Rudnicki, M. A. Muscle satellite cells are multipotential stem cells that exhibit myogenic, osteogenic, and adipogenic differentiation. *Differentiation* **68**, 245–253 (2001).

30. Yin, H. *et al.* MicroRNA-133 controls brown adipose determination in skeletal muscle satellite cells by targeting Prdm16. *Cell Metab* **17**, 210–224 (2013).

31. Dumont, N. A., Wang, Y. X. & Rudnicki, M. A. Intrinsic and extrinsic mechanisms regulating satellite cell function. *Development* **142**, 1572–1581 (2015).

32. Hicks, M. R. & Pyle, A. D. The emergence of the stem cell niche. *Trends Cell Biol* **33**, 112–123 (2023).

33. Deries, M., Gonçalves, A. B. & Thorsteinsdóttir, S. Skeletal Muscle Development: From Stem Cells to Body Movement. in *Springer Nature Switzerland* 159–185 (2020). doi:10.1007/978-3-030-43939-2_9.

34. Bober, E., Franz, T., Arnold, H. H., Gruss, P. & Tremblay, P. Pax-3 is required for the development of limb muscles: A possible role for the migration of dermomyotomal muscle progenitor cells. *Development* **120**, (1994).

35. Tremblay, P. *et al.* A crucial role for Pax3 in the development of the hypaxial musculature and the long-range migration of muscle precursors. *Dev Biol* **203**, (1998).

36. Epstein, J. A., Shapiro, D. N., Cheng, J., Lam, P. Y. P. & Maas, R. L. Pax3 modulates expression of the c-met receptor during limb muscle development. *Proc Natl Acad Sci U S A* **93**, (1996).

37. Oustanina, S., Hause, G. & Braun, T. Pax7 directs postnatal renewal and propagation of myogenic satellite cells but not their specification. *EMBO Journal* **23**, (2004).

38. Relaix, F., Rocancourt, D., Mansouri, A. & Buckingham, M. Divergent functions of murine Pax3 and Pax7 in limb muscle development. *Genes Dev* **18**, (2004).

39. Kuang, S., Chargé, S. B., Seale, P., Huh, M. & Rudnicki, M. A. Distinct roles for Pax7 and Pax3 in adult regenerative myogenesis. *Journal of Cell Biology* **172**, (2006).

40. Relaix, F. *et al.* Pax3 and Pax7 have distinct and overlapping functions in adult muscle progenitor cells. *Journal of Cell Biology* **172**, (2006).

41. Seale, P. *et al.* Pax7 is required for the specification of myogenic satellite cells. *Cell* **102**, (2000).

42. Soleimani, V. D. *et al.* Transcriptional Dominance of Pax7 in Adult Myogenesis Is Due to High-Affinity Recognition of Homeodomain Motifs. *Dev Cell* **22**, (2012).

43. Günther, S. *et al.* Myf5-Positive Satellite Cells Contribute to Pax7-Dependent Long-Term Maintenance of Adult Muscle Stem Cells. *Cell Stem Cell* **13**, (2013).

44. Von Maltzahn, J., Jones, A. E., Parks, R. J. & Rudnicki, M. A. Pax7 is critical for the normal function of satellite cells in adult skeletal muscle. *Proc Natl Acad Sci U S A* **110**, (2013).

45. Hutcheson, D. A., Zhao, J., Merrell, A., Haldar, M. & Kardon, G. Embryonic and fetal limb myogenic cells are derived from developmentally distinct progenitors and have different requirements for β-catenin. *Genes Dev* **23**, (2009).

46. Biressi, S., Molinaro, M. & Cossu, G. Cellular heterogeneity during vertebrate skeletal muscle development. *Developmental Biology* vol. 308 Preprint at https://doi.org/10.1016/j.ydbio.2007.06.006 (2007).

47. Buckingham, M. & Rigby, P. W. J. Gene Regulatory Networks and Transcriptional Mechanisms that Control Myogenesis. *Developmental Cell* vol. 28 Preprint at https://doi.org/10.1016/j.devcel.2013.12.020 (2014).

48. Braun, T., Rudnicki, M. A., Arnold, H. H. & Jaenisch, R. Targeted inactivation of the muscle regulatory gene Myf-5 results in abnormal rib development and perinatal death. *Cell* **71**, (1992).

49. Rudnicki, M. A., Braun, T., Hinuma, S. & Jaenisch, R. Inactivation of MyoD in mice leads to up-regulation of the myogenic HLH gene Myf-5 and results in apparently normal muscle development. *Cell* **71**, (1992).

50. Rudnicki, M. A. *et al.* MyoD or Myf-5 is required for the formation of skeletal muscle. *Cell* **75**, (1993).

51. Hasty, P. *et al.* Muscle deficiency and neonatal death in mice with a targeted mutation in the myogenin gene. *Nature* **364**, (1993).

52. Rawls, A. *et al.* Overlapping functions of the myogenic bHLH genes MRF4 and MyoD revealed in double mutant mice. *Development* **125**, (1998).

53. Zhang, W., Behringer, R. R. & Olson, E. N. Inactivation of the myogenic bHLH gene MRF4 results in up-regulation of myogenin and rib anomalies. *Genes Dev* **9**, (1995).

54. Kassar-Duchossoy, L. *et al.* Pax3/Pax7 mark a novel population of primitive myogenic cells during development. *Genes Dev* **19**, (2005).

55. Relaix, F., Rocancourt, D., Mansouri, A. & Buckingham, M. A Pax3/Pax7-dependent population of skeletal muscle progenitor cells. *Nature* **435**, (2005).

56. Kanisicak, O., Mendez, J. J., Yamamoto, S., Yamamoto, M. & Goldhamer, D. J. Progenitors of skeletal muscle satellite cells express the muscle determination gene, MyoD. *Dev Biol* **332**, (2009).

57. Sousa-Victor, P., García-Prat, L. & Muñoz-Cánoves, P. Control of satellite cell function in muscle regeneration and its disruption in ageing. *Nat Rev Mol Cell Biol* **23**, 204–226 (2022).

58. Fukada, S. I. *et al.* Isolation, characterization, and molecular regulation of muscle stem cells. *Frontiers in Physiology* vol. 4 NOV Preprint at https://doi.org/10.3389/fphys.2013.00317 (2013).

59. van Velthoven, C. T. J. & Rando, T. A. Stem Cell Quiescence: Dynamism, Restraint, and Cellular Idling. *Cell Stem Cell* vol. 24 Preprint at https://doi.org/10.1016/j.stem.2019.01.001 (2019).

60. van Velthoven, C. T. J., de Morree, A., Egner, I. M., Brett, J. O. & Rando, T. A. Transcriptional Profiling of Quiescent Muscle Stem Cells In Vivo. *Cell Rep* **21**, (2017).

61. Machado, L. *et al.* In Situ Fixation Redefines Quiescence and Early Activation of Skeletal Muscle Stem Cells. *Cell Rep* **21**, 1982–1993 (2017).

62. Montarras, D., L'Honoré, A. & Buckingham, M. Lying low but ready for action: the quiescent muscle satellite cell. *FEBS J* **280**, 4036–4050 (2013).

63. Irintchev, A., Zeschnigk, M., Starzinski-Powitz, A. & Wernig, A. Expression pattern of M-cadherin in normal, denervated, and regenerating mouse muscles. *Dev Dyn* **199**, 326–337 (1994).

64. Goel, A. J., Rieder, M. K., Arnold, H. H., Radice, G. L. & Krauss, R. S. Niche Cadherins Control the Quiescence-to-Activation Transition in Muscle Stem Cells. *Cell Rep* **21**, (2017).

65. Pallafacchina, G. *et al.* An adult tissue-specific stem cell in its niche: a gene profiling analysis of in vivo quiescent and activated muscle satellite cells. *Stem Cell Res* **4**, 77–91 (2010).

66. Beauchamp, J. R. *et al.* Expression of CD34 and Myf5 defines the majority of quiescent adult skeletal muscle satellite cells. *Journal of Cell Biology* **151**, (2000).

67. Gnocchi, V. F., White, R. B., Ono, Y., Ellis, J. A. & Zammit, P. S. Further characterisation of the molecular signature of quiescent and activated mouse muscle satellite cells. *PLoS One* **4**, (2009).

68. Eliazer, S. *et al.* Wnt4 from the Niche Controls the Mechano-Properties and Quiescent State of Muscle Stem Cells. *Cell Stem Cell* **25**, (2019).

69. Bjornson, C. R. R. *et al.* Notch signaling is necessary to maintain quiescence in adult muscle stem cells. *Stem Cells* **30**, 232–242 (2012).

70. Philippos, M. *et al.* A critical requirement for notch signaling in maintenance of the quiescent skeletal muscle stem cell state. *Stem Cells* **30**, 243–252 (2012).

71. Mourikis, P. & Tajbakhsh, S. Distinct contextual roles for Notch signalling in skeletal muscle stem cells. *BMC Dev Biol* **14**, (2014).

72. Conboy, I. M. & Rando, T. A. The regulation of Notch signaling controls satellite cell activation and cell fate determination in postnatal myogenesis. *Dev Cell* **3**, 397–409 (2002).

73. Wen, Y. *et al.* Constitutive Notch Activation Upregulates Pax7 and Promotes the Self-Renewal of Skeletal Muscle Satellite Cells. *Mol Cell Biol* **32**, 2300 (2012).

74. Zhou, S., Han, L. & Wu, Z. A Long Journey before Cycling: Regulation of Quiescence Exit in Adult Muscle Satellite Cells. *International Journal of Molecular Sciences* vol. 23 Preprint at https://doi.org/10.3390/ijms23031748 (2022).

75. Buas, M. F., Kabak, S. & Kadesch, T. The notch effector Hey1 associates with myogenic target genes to repress myogenesis. *Journal of Biological Chemistry* **285**, (2010).

76. Chakkalakal, J. V., Jones, K. M., Basson, M. A. & Brack, A. S. The aged niche disrupts muscle stem cell quiescence. *Nature* **490**, (2012).

77. Rodgers, J. T. *et al.* mTORC1 controls the adaptive transition of quiescent stem cells from G0 to G(Alert). *Nature* **510**, 393–396 (2014).

78. Rodgers, J. T., Schroeder, M. D., Ma, C. & Rando, T. A. HGFA Is an Injury-Regulated Systemic Factor that Induces the Transition of Stem Cells into GAlert. *Cell Rep* **19**, (2017).

79. Lee, G. *et al.* Fully reduced HMGB1 accelerates the regeneration of multiple tissues by transitioning stem cells to GAlert. *Proc Natl Acad Sci U S A* **115**, (2018).

80. Der Vartanian, A. *et al.* PAX3 Confers Functional Heterogeneity in Skeletal Muscle Stem Cell Responses to Environmental Stress. *Cell Stem Cell* **24**, (2019).

81. Brun, C. E. *et al.* GLI3 regulates muscle stem cell entry into GAlert and self-renewal. *Nat Commun* **13**, (2022).

82. Fu, X., Wang, H. & Hu, P. Stem cell activation in skeletal muscle regeneration. *Cellular and Molecular Life Sciences* vol. 72 Preprint at https://doi.org/10.1007/s00018-014-1819-5 (2015).

83. Cantini, M. *et al.* Human Satellite Cell-Proliferation in Vitro Is Regulated by Autocrine Secretion of IL-6 Stimulated by a Soluble Factor(s) Released by Activated Monocytes. *Biochem Biophys Res Commun* **216**, (1995).

84. Wang, X. *et al.* Effects of interleukin-6, leukemia inhibitory factor, and ciliary neurotrophic factor on the proliferation and differentiation of adult human myoblasts. *Cell Mol Neurobiol* **28**, (2008).

85. Relaix, F. *et al.* Perspectives on skeletal muscle stem cells. *Nature Communications* vol. 12 Preprint at https://doi.org/10.1038/s41467-020-20760-6 (2021).

86. Rochlin, K., Yu, S., Roy, S. & Baylies, M. K. Myoblast fusion: When it takes more to make one. *Developmental Biology* vol. 341 Preprint at https://doi.org/10.1016/j.ydbio.2009.10.024 (2010).

87. Shirakawa, T. *et al.* Factors Regulating or Regulated by Myogenic Regulatory Factors in Skeletal Muscle Stem Cells. *Cells* vol. 11 Preprint at https://doi.org/10.3390/cells11091493 (2022).

88. Forcina, L., Cosentino, M. & Musarò, A. Mechanisms regulating muscle regeneration: Insights into the interrelated and time-dependent phases of tissue healing. *Cells* vol. 9 Preprint at https://doi.org/10.3390/cells9051297 (2020).

89. Guiraud, S. *et al.* Embryonic myosin is a regeneration marker to monitor utrophin-based therapies for DMD. *Hum Mol Genet* **28**, (2019).

90. Cornelison, D. D. W., Olwin, B. B., Rudnicki, M. A. & Wold, B. J. MyoD(-/-) satellite cells in single-fiber culture are differentiation defective and MRF4 deficient. *Dev Biol* **224**, (2000).

91. Megeney, L. A., Kablar, B., Garrett, K., Anderson, J. E. & Rudnicki, M. A. MyoD is required for myogenic stem cell function in adult skeletal muscle. *Genes Dev* **10**, (1996).

92. Sabourin, L. A., Girgis-Gabardo, A., Scale, P., Asakura, A. & Rudnicki, M. A. Reduced differentiation potential of primary MyoD-/- myogenic cells derived from adult skeletal muscle. *Journal of Cell Biology* **144**, (1999).

93. Park, I. H. & Chen, J. Mammalian target of rapamycin (mTOR) signaling is required for a late-stage fusion process during skeletal myotube maturation. *Journal of Biological Chemistry* **280**, (2005).

94. Park, I. H., Erbay, E., Nuzzi, P. & Chen, J. Skeletal myocyte hypertrophy requires mTOR kinase activity and S6K1. *Exp Cell Res* **309**, (2005).

95. Davie, J. K. *et al.* Target gene selectivity of the myogenic basic helix-loop-helix transcription factor myogenin in embryonic muscle. *Dev Biol* **311**, (2007).

96. Gómez-Gaviro, M. V., Lovell-Badge, R., Fernández-Avilés, F. & Lara-Pezzi, E. The vascular stem cell niche. *J Cardiovasc Transl Res* **5**, (2012).

97. Schmidt, M., Schüler, S. C., Hüttner, S. S., von Eyss, B. & von Maltzahn, J. Adult stem cells at work: regenerating skeletal muscle. *Cellular and Molecular Life Sciences* **76**, 2559–2570 (2019).

98. Garry, G. A., Antony, M. L. & Garry, D. J. Cardiotoxin induced injury and skeletal muscle regeneration. *Methods in Molecular Biology* **1460**, 61–71 (2016).

99. Troy, A. *et al.* Coordination of satellite cell activation and self-renewal by par-complex-dependent asymmetric activation of p38α/β MAPK. *Cell Stem Cell* **11**, (2012).

100. Cheung, T. H. & Rando, T. A. Molecular regulation of stem cell quiescence. *Nature Reviews Molecular Cell Biology* vol. 14 Preprint at https://doi.org/10.1038/nrm3591 (2013).

101. Rocheteau, P., Gayraud-Morel, B., Siegl-Cachedenier, I., Blasco, M. A. & Tajbakhsh, S. A subpopulation of adult skeletal muscle stem cells retains all template DNA strands after cell division. *Cell* **148**, (2012).

102. DiMario, J., Buffinger, N., Yamada, S. & Strohman, R. C. Fibroblast growth factor in the extracellular matrix of dystrophic (mdx) mouse muscle. *Science (1979)* **244**, (1989).

103. Liu, Y. & Schneider, M. F. FGF2 activates TRPC and Ca2+ signaling leading to satellite cell activation. *Front Physiol* **5 FEB**, (2014).

104. Jones, N. C. *et al.* The p38α/β MAPK functions as a molecular switch to activate the quiescent satellite cell. *Journal of Cell Biology* **169**, (2005).

105. Hausburg, M. A. *et al.* Post-transcriptional regulation of satellite cell quiescence by TTP-mediated mRNA decay. *Elife* **2015**, (2015).

106. Segalés, J., Perdiguero, E. & Muñoz-Cánoves, P. Regulation of muscle stem cell functions: A focus on the p38 MAPK signaling pathway. *Frontiers in Cell and Developmental Biology* vol. 4 Preprint at https://doi.org/10.3389/fcell.2016.00091 (2016).

107. Lluís, F., Perdiguero, E., Nebreda, A. R. & Muñoz-Cánoves, P. Regulation of skeletal muscle gene expression by p38 MAP kinases. *Trends in Cell Biology* vol. 16 Preprint at https://doi.org/10.1016/j.tcb.2005.11.002 (2006).

108. Ryall, J. G. *et al.* The NAD+-dependent sirt1 deacetylase translates a metabolic switch into regulatory epigenetics in skeletal muscle stem cells. *Cell Stem Cell* **16**, 171–183 (2015).

109. Pietsch, P. Differentiation in regeneration I. The development of muscle and cartilage following deplantation of regenerating limb blastemata of Amblystoma larvae. *Dev Biol* **3**, (1961).

110. Halevy, O. *et al.* Correlation of Terminal Cell Cycle Arrest of Skeletal Muscle with Induction of p21 by MyoD. *Science (1979)* **267**, (1995).

111. Hollenberg, S. M., Cheng, P. F. & Weintraub, H. Use of a conditional MyoD transcription factor in studies of MyoD trans-activation and muscle determination. *Proc Natl Acad Sci U S A* **90**, (1993).

112. Molkentin, J. D., Black, B. L., Martin, J. F. & Olson, E. N. Cooperative activation of muscle gene expression by MEF2 and myogenic bHLH proteins. *Cell* **83**, (1995).

113. Cserjesi, P. & Olson, E. N. Myogenin induces the myocyte-specific enhancer binding factor MEF-2 independently of other muscle-specific gene products. *Mol Cell Biol* **11**, (1991).

114. Kaushal, S., Schneider, J. W., Nadal-Ginard, B. & Mahdavi, V. Activation of the myogenic lineage by MEF2A, a factor that induces and cooperates with MyoD. *Science (1979)* **266**, (1994).

115. Liu, N. *et al.* Requirement of MEF2A, C, and D for skeletal muscle regeneration. *Proc Natl Acad Sci U S A* **111**, (2014).

116. Brack, A. S., Conboy, I. M., Conboy, M. J., Shen, J. & Rando, T. A. A Temporal Switch from Notch to Wnt Signaling in Muscle Stem Cells Is Necessary for Normal Adult Myogenesis. *Cell Stem Cell* **2**, (2008).

117. Polesskaya, A., Seale, P. & Rudnicki, M. A. Wnt signaling induces the myogenic specification of resident CD45+ adult stem cells during muscle regeneration. *Cell* **113**, (2003).

118. Bentzinger, C. F. *et al.* Fibronectin regulates Wnt7a signaling and satellite cell expansion. *Cell Stem Cell* **12**, (2013).

119. Le Grand, F., Jones, A. E., Seale, V., Scimè, A. & Rudnicki, M. A. Wnt7a Activates the Planar Cell Polarity Pathway to Drive the Symmetric Expansion of Satellite Stem Cells. *Cell Stem Cell* **4**, (2009).

120. Bentzinger, C. F. *et al.* Wnt7a stimulates myogenic stem cell motility and engraftment resulting in improved muscle strength. *Journal of Cell Biology* **205**, (2014).

121. Otto, A. *et al.* Canonical Wnt signalling induces satellite-cell proliferation during adult skeletal muscle regeneration. *J Cell Sci* **121**, (2008).

122. Von Maltzahn, J., Zinoviev, R., Chang, N. C., Bentzinger, C. F. & Rudnicki, M. A. A truncated Wnt7a retains full biological activity in skeletal muscle. *Nat Commun* **4**, (2013).

123. Girardi, F. & Le Grand, F. Wnt Signaling in Skeletal Muscle Development and Regeneration. in *Progress in Molecular Biology and Translational Science* vol. 153 (2018).

124. Von Maltzahn, J., Bentzinger, C. F. & Rudnicki, M. A. Wnt7a-Fzd7 signalling directly activates the Akt/mTOR anabolic growth pathway in skeletal muscle. *Nat Cell Biol* **14**, (2012).

125. von Maltzahn, J., Chang, N. C., Bentzinger, C. F. & Rudnicki, M. A. Wnt signaling in myogenesis. *Trends Cell Biol* **22**, 602–609 (2012).

126. Chen, J. F. *et al.* microRNA-1 and microRNA-206 regulate skeletal muscle satellite cell proliferation and differentiation by repressing Pax7. *Journal of Cell Biology* **190**, (2010).

127. Koning, M., Werker, P. M. N., van Luyn, M. J. A., Krenning, G. & Harmsen, M. C. A global downregulation of microRNAs occurs in human quiescent satellite cells during myogenesis. *Differentiation* **84**, (2012).

128. Dey, B. K., Gagan, J. & Dutta, A. miR-206 and -486 Induce Myoblast Differentiation by Downregulating Pax7. *Mol Cell Biol* **31**, (2011).

129. Koning, M., Werker, P. M. N., Van Der Schaft, D. W. J., Bank, R. A. & Harmsen, M. C. MicroRNA-1 and microRNA-206 Improve differentiation potential of human satellite cells: A novel approach for tissue engineering of skeletal muscle. *Tissue Eng Part A* **18**, (2012).

130. Dalkilic, I., Schienda, J., Thompson, T. G. & Kunkel, L. M. Loss of FilaminC (FLNc) Results in Severe Defects in Myogenesis and Myotube Structure. *Mol Cell Biol* **26**, (2006).

131. Millay, D. P. *et al.* Myomaker is a membrane activator of myoblast fusion and muscle formation. *Nature* **499**, (2013).

132. Millay, D. P., Sutherland, L. B., Bassel-Duby, R. & Olson, E. N. Myomaker is essential for muscle regeneration. *Genes Dev* **28**, (2014).

133. Schwander, M. *et al.* β1 integrins regulate myoblast fusion and sarcomere assembly. *Dev Cell* **4**, (2003).

134. Quach, N. L., Biressi, S., Reichardt, L. F., Keller, C. & Rando, T. A. Focal adhesion kinase signaling regulates the expression of caveolin 3 and β1 integrin, genes essential for normal myoblast fusion. *Mol Biol Cell* **20**, (2009).

135. Tadokoro, S. *et al.* Talin binding to integrin β tails: A final common step in integrin activation. *Science (1979)* **302**, (2003).

136. Horsley, V., Jansen, K. M., Mills, S. T. & Pavlath, G. K. IL-4 acts as a myoblast recruitment factor during mammalian muscle growth. *Cell* **113**, (2003).

137. Clark, P., Coles, D. & Peckham, M. Preferential adhesion to and survival on patterned laminin organizes myogenesis in vitro. *Exp Cell Res* **230**, (1997).

138. Rommel, C. *et al.* Mediation of IGF-1-induced skeletal myotube hypertrophy by Pl(3)K/Alt/mTOR and Pl(3)K/Akt/GSK3 pathways. *Nat Cell Biol* **3**, (2001).

139. Bassel-Duby, R. & Olson, E. N. Signaling pathways in skeletal muscle remodeling. *Annual Review of Biochemistry* vol. 75 Preprint at https://doi.org/10.1146/annurev.biochem.75.103004.142622 (2006).

140. Sandri, M. *et al.* Foxo transcription factors induce the atrophy-related ubiquitin ligase atrogin-1 and cause skeletal muscle atrophy. *Cell* **117**, (2004).

141. Feige, P., Brun, C. E., Ritso, M. & Rudnicki, M. A. Orienting Muscle Stem Cells for Regeneration in Homeostasis, Aging, and Disease. *Cell Stem Cell* vol. 23 Preprint at https://doi.org/10.1016/j.stem.2018.10.006 (2018).

142. Kawabe, Y. I., Wang, Y. X., McKinnell, I. W., Bedford, M. T. & Rudnicki, M. A. Carm1 regulates Pax7 transcriptional activity through MLL1/2 recruitment during asymmetric satellite stem cell divisions. *Cell Stem Cell* **11**, (2012).

143. McKinnell, I. W. *et al.* Pax7 activates myogenic genes by recruitment of a histone methyltransferase complex. *Nat Cell Biol* **10**, (2008).

144. Yennek, S., Burute, M., Théry, M. & Tajbakhsh, S. Cell adhesion geometry regulates non-random DNA segregation and asymmetric cell fates in mouse skeletal muscle stem cells. *Cell Rep* **7**, (2014).

145. Shinin, V., Gayraud-Morel, B., Gomès, D. & Tajbakhsh, S. Asymmetric division and cosegregation of template DNA strands in adult muscle satellite cells. *Nat Cell Biol* **8**, (2006).

146. Shea, K. L. *et al.* Sprouty1 Regulates Reversible Quiescence of a Self-Renewing Adult Muscle Stem Cell Pool during Regeneration. *Cell Stem Cell* **6**, (2010).

147. Lukjanenko, L. *et al.* Aging Disrupts Muscle Stem Cell Function by Impairing Matricellular WISP1 Secretion from Fibro-Adipogenic Progenitors. *Cell Stem Cell* **24**, (2019).

148. Brack, A. S. & Muñoz-Cánoves, P. The ins and outs of muscle stem cell aging. *Skeletal Muscle* vol. 6 Preprint at https://doi.org/10.1186/s13395-016-0072-z (2016).

149. Brack, A. S. *et al.* Increased Wnt signaling during aging alters muscle stem cell fate and increases fibrosis. *Science (1979)* **317**, (2007).

150. Chang, N. C., Chevalier, F. P. & Rudnicki, M. A. Satellite Cells in Muscular Dystrophy - Lost in Polarity. *Trends in Molecular Medicine* vol. 22 Preprint at https://doi.org/10.1016/j.molmed.2016.04.002 (2016).

151. Kottlors, M. & Kirschner, J. Elevated satellite cell number in Duchenne muscular dystrophy. *Cell Tissue Res* **340**, (2010).

152. Bankolé, L. C., Feasson, L., Ponsot, E. & Kadi, F. Fibre type-specific satellite cell content in two models of muscle disease. *Histopathology* **63**, (2013).

153. Dumont, N. A. *et al.* Dystrophin expression in muscle stem cells regulates their polarity and asymmetric division. *Nat Med* **21**, (2015).

154. Ahlqvist, K. J. *et al.* Stem cells, mitochondria and aging. *Biochim Biophys Acta Bioenerg* **1847**, 1380–1386 (2015).

155. Cairns, G., Thumiah-Mootoo, M., Burelle, Y. & Khacho, M. Mitophagy: A new player in stem cell biology. *Biology (Basel)* **9**, 1–24 (2020).

156. Zhang, H., Menzies, K. J. & Auwerx, J. The role of mitochondria in stem cell fate and aging. *Development (Cambridge)* **145**, (2018).

157. Zhang, F. *et al.* P53 and Parkin co-regulate mitophagy in bone marrow mesenchymal stem cells to promote the repair of early steroid-induced osteonecrosis of the femoral head. *Cell Death Dis* **11**, (2020).

158. Correia-Melo, C. *et al.* Mitochondria are required for pro-ageing features of the senescent phenotype. *EMBO J* **35**, (2016).

159. Zhang, J., Nuebel, E., Daley, G. Q., Koehler, C. M. & Teitell, M. A. Metabolic regulation in pluripotent stem cells during reprogramming and self-renewal. *Cell Stem Cell* **11**, 589–595 (2012).

160. Chen, Y., McMillan-Ward, E., Kong, J., Israels, S. J. & Gibson, S. B. Mitochondrial electron-transport-chain inhibitors of complexes I and II induce autophagic cell death mediated by reactive oxygen species. *J Cell Sci* **120**, (2007).

161. Choksi, K. B., Nuss, J. E., Boylston, W. H., Rabek, J. P. & Papaconstantinou, J. Age-related increases in oxidatively damaged proteins of mouse kidney mitochondrial electron transport chain complexes. *Free Radic Biol Med* **43**, (2007).

162. Khacho, M. *et al.* Mitochondrial Dynamics Impacts Stem Cell Identity and Fate Decisions by Regulating a Nuclear Transcriptional Program. *Cell Stem Cell* **19**, 232–247 (2016).

163. Papa, L., Djedaini, M. & Hoffman, R. Mitochondrial role in stemness and differentiation of hematopoietic stem cells. *Stem Cells Int* **2019**, (2019).

164. Khacho, M. & Slack, R. S. Mitochondrial and reactive oxygen species signaling coordinate stem cell fate decisions and life long maintenance. *Antioxid Redox Signal* **28**, 1090–1101 (2018).

165. Liang, R. *et al.* Restraining Lysosomal Activity Preserves Hematopoietic Stem Cell Quiescence and Potency. *Cell Stem Cell* **26**, 359-376.e7 (2020).

166. Lisowski, P., Kannan, P., Mlody, B. & Prigione, A. Mitochondria and the dynamic control of stem cell homeostasis. *EMBO Rep* **19**, (2018).

167. Seo, B. J., Yoon, S. H. & Do, J. T. Mitochondrial Dynamics in Stem Cells and Differentiation. *Int J Mol Sci* **19**, (2018).

168. Fu, W., Liu, Y. & Yin, H. Mitochondrial dynamics: Biogenesis, fission, fusion, and mitophagy in the regulation of stem cell behaviors. *Stem Cells International* vol. 2019 Preprint at https://doi.org/10.1155/2019/9757201 (2019).

169. Baker, N. *et al.* The mitochondrial protein OPA1 regulates the quiescent state of adult muscle stem cells. *Cell Stem Cell* **29**, 1315-1332.e9 (2022).

170. Ryall, J. G., Cliff, T., Dalton, S. & Sartorelli, V. Metabolic Reprogramming of Stem Cell Epigenetics. *Cell Stem Cell* **17**, 651–662 (2015).

171. Ito, K. & Suda, T. Metabolic requirements for the maintenance of self-renewing stem cells. *Nat Rev Mol Cell Biol* **15**, 243–256 (2014).

172. Schell, J. C. *et al.* Control of intestinal stem cell function and proliferation by mitochondrial pyruvate metabolism. *Nat Cell Biol* **19**, 1027–1036 (2017).

173. Wei, P., Dove, K. K., Bensard, C., Schell, J. C. & Rutter, J. The Force Is Strong with This One: Metabolism (Over)powers Stem Cell Fate. *Trends Cell Biol* **28**, 551–559 (2018).

174. Folmes, C. D. L. *et al.* Somatic oxidative bioenergetics transitions into pluripotency-dependent glycolysis to facilitate nuclear reprogramming. *Cell Metab* **14**, 264–271 (2011).

175. Varum, S. *et al.* Energy metabolism in human pluripotent stem cells and their differentiated counterparts. *PLoS One* **6**, (2011).

176. Flores, A. *et al.* Lactate dehydrogenase activity drives hair follicle stem cell activation. *Nat Cell Biol* **19**, 1017–1026 (2017).

177. Khacho, M. & Slack, R. S. Mitochondrial activity in the regulation of stem cell self-renewal and differentiation. *Curr Opin Cell Biol* **49**, 1–8 (2017).

178. Ren, R., Ocampo, A., Liu, G. H. & Izpisua Belmonte, J. C. Regulation of Stem Cell Aging by Metabolism and Epigenetics. *Cell Metab* **26**, 460–474 (2017).

179. Brunet, A. & Rando, T. A. Interaction between epigenetic and metabolism in aging stem cells. *Curr Opin Cell Biol* **45**, 1–7 (2017).

180. Wellen, K. E. *et al.* ATP-citrate lyase links cellular metabolism to histone acetylation. *Science (1979)* **324**, 1076–1080 (2009).

181. Sørensen, A. L. *et al.* Lineage-specific promoter DNA methylation patterns segregate adult progenitor cell types. *Stem Cells Dev* **19**, 1257–1266 (2010).

182. Hwang, I. Y. *et al.* Psat1-Dependent Fluctuations in α-Ketoglutarate Affect the Timing of ESC Differentiation. *Cell Metab* **24**, 494–501 (2016).

183. Carey, B. W., Finley, L. W. S., Cross, J. R., Allis, C. D. & Thompson, C. B. Intracellular α-ketoglutarate maintains the pluripotency of embryonic stem cells. *Nature* **518**, 413–416 (2015).

184. Gong, G. *et al.* Parkin-mediated mitophagy directs perinatal cardiac metabolic maturation in mice. *Science (1979)* **350**, (2015).

185. Piquereau, J. *et al.* Postnatal development of mouse heart: formation of energetic microdomains. *J Physiol* **588**, 2443–2454 (2010).

186. Seyer, P. *et al.* Mitochondrial activity regulates myoblast differentiation by control of c-Myc expression. *J Cell Physiol* **207**, 75–86 (2006).

187. Rochard, P. *et al.* Mitochondrial activity is involved in the regulation of myoblast differentiation through myogenin expression and activity of myogenic factors. *Journal of Biological Chemistry* **275**, 2733–2744 (2000).

188. Triolo, M. *et al.* Optic atrophy 1 mediates muscle differentiation by promoting a metabolic switch via the supercomplex assembly factor SCAF1. *iScience* **27**, (2024).

189. Ng, M. Y. W., Wai, T. & Simonsen, A. Quality control of the mitochondrion. *Developmental Cell* vol. 56 Preprint at https://doi.org/10.1016/j.devcel.2021.02.009 (2021).

190. VJJ, C., G, V., KJ, M. & Y, B. Mitochondrial quality control in the cardiac system: An integrative view. *Biochim Biophys Acta Mol Basis Dis* **1865**, 782–796 (2019).

191. Dikic, I. & Elazar, Z. Mechanism and medical implications of mammalian autophagy. *Nature Reviews Molecular Cell Biology* vol. 19 Preprint at https://doi.org/10.1038/s41580-018-0003-4 (2018).

192. Boya, P., Codogno, P. & Rodriguez-Muela, N. Autophagy in stem cells: repair, remodelling and metabolic reprogramming. *Development* **145**, (2018).

193. Leduc-Gaudet, J. P., Reynaud, O., Hussain, S. N. & Gouspillou, G. Parkin overexpression protects from ageing-related loss of muscle mass and strength. *Journal of Physiology* **597**, 1975–1991 (2019).

194. Narendra, D., Tanaka, A., Suen, D. F. & Youle, R. J. Parkin is recruited selectively to impaired mitochondria and promotes their autophagy. *Journal of Cell Biology* **183**, 795–803 (2008).

195. Dorn, G. W. & Kitsis, R. N. The mitochondrial dynamism-mitophagy-cell death interactome: Multiple roles performed by members of a mitochondrial molecular ensemble. *Circulation Research* vol. 116 Preprint at https://doi.org/10.1161/CIRCRESAHA.116.303554 (2015).

196. Mizushima, N. & Komatsu, M. Autophagy: Renovation of Cells and Tissues. *Cell* **147**, 728–741 (2011).

197. Kim, I. & Lemasters, J. J. Mitochondrial degradation by autophagy (mitophagy) in GFP-LC3 transgenic hepatocytes during nutrient deprivation. *Am J Physiol Cell Physiol* **300**, (2011).

198. Lemasters, J. J. Selective mitochondrial autophagy, or mitophagy, as a targeted defense against oxidative stress, mitochondrial dysfunction, and aging. *Rejuvenation Res* **8**, 3–5 (2005).

199. García-Prat, L., Martínez-Vicente, M. & Muñoz-Cánoves, P. Methods for mitochondria and mitophagy flux analyses in stem cells of resting and regenerating skeletal muscle. in *Methods in Molecular Biology* vol. 1460 (2016).

200. Johansen, T. & Lamark, T. Selective Autophagy: ATG8 Family Proteins, LIR Motifs and Cargo Receptors. *Journal of Molecular Biology* vol. 432 Preprint at https://doi.org/10.1016/j.jmb.2019.07.016 (2020).

201. Jin, S. M. *et al.* Mitochondrial membrane potential regulates PINK1 import and proteolytic destabilization by PARL. *Journal of Cell Biology* **191**, 933–942 (2010).

202. Narendra, D. P. *et al.* PINK1 is selectively stabilized on impaired mitochondria to activate Parkin. *PLoS Biol* **8**, (2010).

203. Jin, S. M. & Youle, R. J. The accumulation of misfolded proteins in the mitochondrial matrix is sensed by PINK1 to induce PARK2/Parkin-mediated mitophagy of polarized mitochondria. *Autophagy* **9**, (2013).

204. Kim, Y. *et al.* PINK1 controls mitochondrial localization of Parkin through direct phosphorylation. *Biochem Biophys Res Commun* **377**, 975–980 (2008).

205. Kane, L. A. *et al.* PINK1 phosphorylates ubiquitin to activate parkin E3 ubiquitin ligase activity. *Journal of Cell Biology* **205**, 143–153 (2014).

206. Koyano, F. *et al.* Ubiquitin is phosphorylated by PINK1 to activate parkin. *Nature* **510**, 162–166 (2014).

207. Kazlauskaite, A. *et al.* Phosphorylation of parkin at serine65 is essential for activation: Elaboration of a miro1 substrate-based assay of parkin E3 ligase activity. *Open Biol* **4**, (2014).

208. Kane, L. A. & Youle, R. J. PINK1 and Parkin flag miro to direct mitochondrial traffic. *Cell* vol. 147 Preprint at https://doi.org/10.1016/j.cell.2011.10.028 (2011).

209. Chen, Y. & Dorn, G. W. PINK1-phosphorylated mitofusin 2 is a parkin receptor for culling damaged mitochondria. *Science (1979)* **340**, (2013).

210. Gegg, M. E. *et al.* Mitofusin 1 and mitofusin 2 are ubiquitinated in a PINK1/parkin-dependent manner upon induction of mitophagy. *Hum Mol Genet* **19**, (2010).

211. Poole, A. C., Thomas, R. E., Yu, S., Vincow, E. S. & Pallanck, L. The mitochondrial fusion-promoting factor mitofusin is a substrate of the PINK1/parkin pathway. *PLoS One* **5**, (2010).

212. Glauser, L., Sonnay, S., Stafa, K. & Moore, D. J. Parkin promotes the ubiquitination and degradation of the mitochondrial fusion factor mitofusin 1. *J Neurochem* **118**, (2011).

213. Kirkin, V. *et al.* A Role for NBR1 in Autophagosomal Degradation of Ubiquitinated Substrates. *Mol Cell* **33**, (2009).

214. Lee, J. Y., Nagano, Y., Taylor, J. P., Lim, K. L. & Yao, T. P. Disease-causing mutations in Parkin impair mitochondrial ubiquitination, aggregation, and HDAC6-dependent mitophagy. *Journal of Cell Biology* **189**, (2010).

215. Pankiv, S. *et al.* p62/SQSTM1 binds directly to Atg8/LC3 to facilitate degradation of ubiquitinated protein aggregates by autophagy*[S]. *Journal of Biological Chemistry* **282**, (2007).

216. Cairns, G. *et al.* PINK1 Deficiency Alters Muscle Stem Cell Fate Decision and Muscle Regenerative Capacity. *bioRxiv* (2023).

217. Palikaras, K., Lionaki, E. & Tavernarakis, N. Mechanisms of mitophagy in cellular homeostasis, physiology and pathology. *Nature Cell Biology 2018 20:9* **20**, 1013–1022 (2018).

218. GeneCard. BNIP3L Gene - BCL2 Interacting Protein 3 Like. https://www.genecards.org/cgi-bin/carddisp.pl?gene=BNIP3L.

219. National Center for Biotechnology Information. BNIP3L BCL2 interacting protein 3 like [Homo sapiens (human)]. (2021).

220. Chen, Y. *et al.* A nucleus-targeted alternately spliced Nix/Bnip3L protein isoform modifies nuclear factor κB (NFκB)-mediated cardiac transcription. *Journal of Biological Chemistry* **288**, (2013).

221. Chen, G. *et al.* Nix and Nip3 form a subfamily of pro-apoptotic mitochondrial proteins. *Journal of Biological Chemistry* **274**, (1999).

222. Schweers, R. L. *et al.* NIX is required for programmed mitochondrial clearance during reticulocyte maturation. *Proc Natl Acad Sci U S A* **104**, 19500–19505 (2007).

223. Diwan, A. *et al.* Unrestrained erythroblast development in Nix-/- mice reveals a mechanism for apoptotic modulation of erythropoiesis. *Proc Natl Acad Sci U S A* **104**, 6794–6799 (2007).

224. Aerbajinai, W., Giattina, M., Lee, Y. T., Raffeld, M. & Miller, J. L. The proapoptotic factor Nix is coexpressed with Bcl-xL during terminal erythroid differentiation. *Blood* **102**, (2003).

225. Marinković, M., Šprung, M. & Novak, I. Dimerization of mitophagy receptor BNIP3L/NIX is essential for recruitment of autophagic machinery. *Autophagy* **17**, 1232–1243 (2021).

226. Yang, Z. & Klionsky, D. J. Mammalian autophagy: Core molecular machinery and signaling regulation. *Current Opinion in Cell Biology* vol. 22 Preprint at https://doi.org/10.1016/j.ceb.2009.11.014 (2010).

227. Novak, I. *et al.* Nix is a selective autophagy receptor for mitochondrial clearance. *EMBO Rep* **11**, 45–51 (2010).

228. Gao, F. *et al.* The mitochondrial protein BNIP3L is the substrate of PARK2 and mediates mitophagy in PINK1/PARK2 pathway. *Hum Mol Genet* **24**, 2528–2538 (2015).

229. Rogov, V. V. *et al.* Phosphorylation of the mitochondrial autophagy receptor Nix enhances its interaction with LC3 proteins. *Sci Rep* **7**, (2017).

230. Bruick, R. K. Expression of the gene encoding the proapoptotic Nip3 protein is induced by hypoxia. *Proc Natl Acad Sci U S A* **97**, (2000).

231. Sowter, H. M., Ratcliffe, P. J., Watson, P., Greenberg, A. H. & Harris, A. L. HIF-1-dependent regulation of hypoxic induction of the cell death factors BNIP3 and NIX in human tumors. *Cancer Res* **61**, (2001).

232. Murphy, M. M., Lawson, J. A., Mathew, S. J., Hutcheson, D. A. & Kardon, G. Satellite cells, connective tissue fibroblasts and their interactions are crucial for muscle regeneration. *Development* **138**, (2011).

233. Parise, G., McKinnell, I. W. & Rudnicki, M. A. Muscle satellite cell and atypical myogenic progenitor response following exercise. *Muscle Nerve* **37**, (2008).

234. Sincennes, M. C., Wang, Y. X. & Rudnicki, M. A. Primary mouse myoblast purification using magnetic cell separation. in *Methods in Molecular Biology* vol. 1556 (2017).

235. Lambert, R. *et al.* Breeding Strategies for Maintaining Colonies of Laboratory Mice, A Jackson Laboratory Resource Manual. *The Jackson Laboratory* (2009).

236. Gendron, W. A. C. *et al.* Unlocking loxp to track genome editing in vivo. *Genes (Basel)* **12**, (2021).

237. Killackey, S. A., Philpott, D. J. & Girardin, S. E. Mitophagy pathways in health and disease. *J Cell Biol* **219**, (2020).

238. Booth, F. W., Ruegsegger, G. N., Toedebusch, R. G. & Yan, Z. Endurance Exercise and the Regulation of Skeletal Muscle Metabolism. doi:10.1016/bs.pmbts.2015.07.016.